# CD14 release induced by P2X7 receptor restrict inflammation and increases survival during sepsis

Cristina Alarcón-Vila[1], Alberto Baroja-Mazo[1†], Carlos de Torre-Minguela[1†], Carlos M. Martínez[2], Juan J. Martínez-García[1,‡], Helios Martínez-Banaclocha[1], Carlos García-Palenciano[3] and Pablo Pelegrín[1*]

[1]Línea de Inflamación Molecular, Instituto Murciano de Investigación Biosanitaria IMIB-Arrixaca, Hospital Clínico Universitario Virgen de la Arrixaca, Murcia, Spain.

[2]Plataforma de Patología, Instituto Murciano de Investigación Biosanitaria IMIB-Arrixaca, Murcia, Spain.

[3]Unidad de Reanimación, Hospital Clínico Universitario Virgen de la Arrixaca, Murcia, Spain.

[†]These authors contributed equally to this work.

[‡]Present address: U1003 Phycell lab; Inflammasome and Ion channels; Université de Lille; INSERM; Institut Pasteur de Lille, F-59000, Lille, France.

*Correspondence: Dr. Pablo Pelegrín. Edificio LAIB 4ª Planta, Instituto Murciano de Investigación Biosanitaria (IMIB-Arrixaca). Carretera Buenavista s/n. 30120 El Palmar, Murcia, Spain. Phone number: +34 868 885 038; e-mail: pablo.pelegrin@imib.es

**RUNNING TITLE**: P2X7 receptor controls CD14 release during sepsis.

**IMPACT STATEMENT:** A murine model of sepsis shows that the purinergic P2X7 receptor controls the release of CD14 in extracellular vesicles which plays a key role in cytokine production, bacterial clearance and survival during sepsis.

**ABSTRACT**

P2X7 receptor activation induces the release of different cellular proteins, such as CD14, a glycosylphosphatidylinositol (GPI)-anchored protein to the plasma membrane important for LPS signaling via TLR4. Circulating CD14 has been found at elevated levels in sepsis, but the exact mechanism of CD14 release in sepsis has not been established. Here we show for first time that P2X7 receptor induces the release of CD14 in extracellular vesicles, resulting in a net reduction in macrophage plasma membrane CD14 that functionally affects LPS, but not monophosphoryl lipid A, pro-inflammatory cytokine production. Also, we found that during a murine model of sepsis, P2X7 receptor activity is important for maintaining elevated levels of CD14 in biological fluids and a decrease in its activity results in higher bacterial load and exacerbated organ damage, ultimately leading to premature deaths. Our data reveal that P2X7 is a key receptor for helping to clear sepsis because it maintains elevated concentrations of circulating CD14 during infection.

39 **INTRODUCTION**

40 Purinergic signaling controls many different processes during infection and inflammation
41 (Eltzschig et al., 2012) and the P2X7 receptor is one of the key purinergic receptors in
42 modulating the macrophage functions that orchestrate the inflammatory response (Di
43 Virgilio et al., 2017). The P2X7 receptor in LPS-primed macrophages activates the
44 nucleotide-binding domain and the leucine-rich repeat receptor pyrin domain containing
45 3 (NLRP3) inflammasome, which in turn leads to the release of pro-inflammatory
46 cytokines from the interleukin (IL)-1 family, such as IL-1β (Di Virgilio et al., 2017).
47 However, the P2X7 receptor can also block NLRP3 if it is activated before the LPS
48 priming of the macrophages (Martínez-García et al., 2019). This means that the P2X7
49 receptor can cause different pro- or anti-inflammatory responses depending when it is
50 activated. In macrophages, the P2X7 receptor also induces the release of extracellular
51 vesicles that contain IL-1β and MHCII (MacKenzie et al., 2001; Pellegatti et al., 2008; Qu
52 et al., 2009, 2007); however, apart from these proteins, the cargo of P2X7 receptor-
53 induced extracellular vesicles, remains largely unknown. A large fraction of IL-1β and
54 other cytosolic proteins are also released via pyroptosis, a type of cell death dependent
55 on inflammasome activation and the formation of large plasma membrane pores by
56 gasdermin D (Broz et al., 2020).The secretome of the P2X7 receptor in macrophages
57 includes many soluble proteins released by pyroptosis and some prototypic proteins of
58 extracellular vesicles, such as annexin A1 (de Torre-Minguela et al., 2016). One of the
59 plasma membrane-associated proteins identified as part of the P2X7 receptor secretome
60 is CD14, a well-known myeloid cell marker (de Torre-Minguela et al., 2016; Setoguchi et
61 al., 1989). CD14 is a glycosylphosphatidylinositol (GPI)-anchored membrane protein
62 important for transferring LPS to Toll-like receptor (TLR) 4 and for controlling TLR4
63 translocation to endosomes that activate TRAM-TRIF-dependent pathways (Zanoni et
64 al., 2013). Therefore, CD14 is important for ensuring that TLR4 responds optimally to
65 LPS and that macrophages produce pro-inflammatory cytokines. CD14 could be

66 released from the cells by the action of proteinase (Wu et al., 2019), however there are
67 also different release mechanism independent of proteinase that are not known. The
68 pool of extracellular CD14 *in vivo*, known as soluble CD14, is detected in different fluids
69 during infection and particularly during sepsis, a life-threating condition resulting from
70 exacerbated inflammation in response to infection (Barratt-Due et al., 2017; Bas et al.,
71 2004). Extracellular CD14 during microbial infection is important for host defense, in
72 particular for bacterial clearance, but little is known about the release of CD14 *in vivo*
73 (Fang et al., 2017; Knapp et al., 2006; Sahay et al., 2018; Wieland et al., 2005). Despite
74 the fact that the P2X7 receptor induces the release of CD14 (de Torre-Minguela et al.,
75 2016), it is not known if P2X7 contributes to the extracellular pool of CD14 during
76 infection or what its role is in defending the host during sepsis. In this study, we found
77 for first time that CD14 is a cargo of extracellular vesicles released by P2X7 receptor
78 activation and functionally that the lack of cellular CD14 compromises the production of
79 macrophage pro-inflammatory cytokines. Additionally, we also found that during sepsis
80 there is a decrease in the extracellular pool of CD14 in *P2rx7*$^{-/-}$ mice, which results in
81 high bacterial dissemination and a decreased mice survival and reveals that the P2X7
82 receptor is important for maintaining an optimum level of CD14 and thus ensuring
83 survival of sepsis.

84 **RESULTS**

85 **P2X7 receptor stimulation induces the release of extracellular vesicles containing**
86 **CD14**

87 In a previous study, we identified CD14 as a specific component of the P2X7 receptor
88 secretome in macrophages (de Torre-Minguela et al., 2016). After ATP stimulation of
89 LPS-primed macrophages, we detected the appearance of extracellular CD14 in the
90 100K pellet together with the tetraspanin CD9, a well-known extracellular vesicle marker
91 (Figure 1a). This pellet contained extracellular vesicles with an average size of 167.4 nm
92 (Figure 1-supplement 1a). Most of the P2X7 receptor secretome examined, with the
93 exception of IL-1β, was present in the soluble fraction and not associated with the 100K
94 pellet (Figure 1-supplement 1b).The presence of CD14 in extracellular vesicles obtained
95 from macrophage supernatants after P2X7 receptor stimulation was also determined by
96 using a protocol for extracellular vesicle isolation based in polymer-precipitation (Figure
97 1b). The treatment of whole cellular supernatants with Triton X100 before vesicle
98 isolation resulted in a loss of CD14 from the100K pellet fraction that was detected in the
99 soluble fraction (100K supernatant) (Figure 1c), suggesting CD14 is a cargo of the
100 vesicles. The CD14 in the 100K pellet was detected just after 5 min of ATP stimulation
101 (Figure 1-supplement 1c) and was independent of the macrophage activation polarity,
102 as it was detected from M1 and M2 macrophages (Figure 1d). However the number of
103 extracellular vesicles released in LPS-primed macrophages (M1) after P2X7 receptor
104 stimulation was significantly higher than those released from IL-4 treated (M2) or resting
105 macrophages (Figure 1e-supplement 2a). Interestingly, the release of CD14 induced by
106 the P2X7 receptor in extracellular vesicles was highly dependent on the NLRP3
107 inflammasome, but not on caspase-1 (Figure 1f). Then we found that the amount of
108 extracellular vesicles released after activation of the P2X7 receptor in *Nlrp3*$^{-/-}$ and
109 *Casp1/11*$^{-/-}$ macrophages was smaller when compared with wild type macrophages
110 (Figure1g-supplement 2b). The morphology of *Nlrp3*$^{-/-}$-derived extracellular vesicles was

111 similar to that of resting or IL-4-primed wild-type macrophages (Figure 1-supplement
112 2a,b). In contrast, *Casp1/11*$^{-/-}$-derived extracellular vesicles were similar in morphology
113 to LPS-primed wild-type macrophages (Figure 1-supplement 2a,b), indicating that a
114 specific pool of extracellular vesicle-dependent on LPS-priming and NLRP3 could be
115 enriched in CD14 and explain the differences of released CD14 found among *Nlrp3*$^{-/-}$
116 and *Casp1/11*$^{-/-}$ macrophages. The release of CD14 observed in ATP-treated
117 macrophages resulted in a significant decrease in cell surface CD14 (Figure 1h), thus
118 suggesting that the P2X7 receptor could induce a decrease in CD14-dependent signaling
119 in macrophages as well as being a source of extracellular CD14.

120

121 **P2X7 receptor stimulation impairs LPS-mediated signaling**

122 CD14 is a co-receptor of TLR4 important for LPS signaling (Zanoni et al., 2013), so we
123 investigated whether CD14 released after P2X7 receptor activation affect the signaling
124 of LPS in macrophages. Treatment of macrophages with extracellular ATP and then
125 subjected to LPS activation resulted in a decrease in LPS-induced expression and a
126 secretion of the pro-inflammatory cytokines IL-6 and TNF-α (Figure 2a,b). This effect was
127 abrogated when the specific P2X7 receptor antagonist A438079 was used or when
128 macrophages were isolated from *P2rx7*$^{-/-}$ mice (Figure 2a,b), thus suggesting that the
129 P2X7 receptor was affecting LPS signaling in macrophages. LPS is not able to activate
130 TLR4 in the absence of CD14 at the cell membrane (Pizzuto et al., 2018). By contrast,
131 lipopolysaccharides with smaller hydrophilic moiety, like monophosphoryl lipid A (MPLA),
132 signals independently of CD14 (Maeshima and Fernandez, 2013). In order to investigate
133 the role of P2X7 receptor-induced CD14 release in the reduction of LPS signaling, we
134 tested whether also MPLA signaling was impaired by P2X7 receptor activation. When
135 macrophages were stimulated with MPLA the production of IL-6 and TNF-α was not
136 affected when P2X7 receptor was activated (Figure 2c,d). This effect was similar when

137 CD14 was blocked with a specific antibody; when this was done, it decreased the
138 production of both cytokines after LPS was added to stimulate the macrophages but not
139 when MPLA was used (Figure 2-supplement 1a,b). Our group has recently reported that
140 in macrophages, activating the P2X7 receptor before LPS-priming also inhibits NLRP3
141 inflammasome, a phenomena mediated by P2X7 receptor-mediated mitochondrial
142 damage (Martínez-García et al., 2019). To assess the possible involvement of CD14
143 release in NLRP3 inhibition we first measured *Il1b* gene expression and found that,
144 similarly to *Il6* and *Tnfa*, ATP treatment decreased the expression of *Il1b* when LPS was
145 used to activate the cells, but not when MPLA was used (Figure 2e), suggesting that the
146 decrease of CD14 on cell membrane affects the priming by LPS. However, the release
147 of IL-1β induced by nigericin decreased when macrophages were incubated with ATP
148 before LPS- or MPLA-priming (Figure 2f), which suggests that *Il1b* production, but not
149 NLRP3 activation, was affected by the release of CD14 induced by the activation of the
150 P2X7 receptor.

151

152 **P2X7 receptor controls CD14 in extracellular vesicles during sepsis**

153 The extracellular pool of CD14 increases during infection and sepsis (Bas et al., 2004),
154 and here we confirm that septic patients presented elevated levels of CD14 in the plasma
155 when compared to non-septic volunteers (Figure 3a and Supplementary File 1-Table 1).
156 Similarly, the presence of P2X7 receptor in monocytes was also elevated in septic
157 individuals (Figure 3a), in accordance to previous studies (Martínez-García et al., 2019).
158 To study if P2X7 receptor is important in maintaining the extracellular pool of CD14
159 during infection, we performed the cecal ligation and puncture (CLP) procedure in
160 *P2rx7*$^{-/-}$ mice and we found that the lack of P2X7 receptor expression resulted in reduced
161 levels of cell-free CD14 in both serum and peritoneal lavage (Figure 3b). Similarly,
162 administration of the specific P2X7-receptor-antagonist A438079 to wild-type mice

163 subjected to CLP resulted in a reduction in CD14 in the peritoneal lavage and a mild
164 reduction in serum (Figure 3c). This result could be probably due to the site of A438079
165 injection, which was i.p., and to its short half-life, which hampers its ability to reach the
166 blood serum (McGaraughty et al., 2007). Furthermore, the increase in CD14 detected in
167 the peritoneal lavage was mainly associated with the extracellular vesicle pool (Figure
168 3d), and the presence of CD14 in extracellular vesicles decreased in P2X7-receptor
169 deficient mice (Figure 3d). These data suggest that during infection, the P2X7 receptor
170 contribute to the presence of extracellular CD14 in extracellular vesicles.

171

172 **Deficiency in the P2X7 receptor increases cytokine production during sepsis**

173 In order to determine if the P2X7-receptor-dependent release of CD14 during sepsis was
174 impairing LPS-signaling *in vivo*, we measured cytokines in the serum of P2X7-deficient
175 mice subjected to CLP. In line with our *in vitro* data, levels of IL-6 appeared higher in the
176 *P2rx7*$^{-/-}$ mice after CLP compared to wild-type (Figure 4a). This was also confirmed for
177 other cytokines, chemokines and acute phase proteins measured in the serum of
178 *P2rx7*$^{-/-}$ mice as well as in wild-type mice treated with A438079 (Figure 4b,c), which
179 suggests that P2X7 receptor is important for the downregulation of cytokines during
180 sepsis.

181

182 **Extracellular CD14 induced by the P2X7 receptor during sepsis controls bacterial**
183 **dissemination and cytokine secretion**

184 In order to elucidate if extracellular CD14 released by P2X7 has a role during sepsis, we
185 next analyzed bacterial dissemination, as it is known that extracellular CD14 contributes
186 to the clearance of invading bacteria and that the P2X7 receptor is important for
187 controlling bacterial content during sepsis (Csóka et al., 2015; Lévêque et al., 2017). As

188 expected, the bacterial burden increased in serum, peritoneal cavity and liver in *P2rx7*$^{-/-}$
189 compared to wild-type mice after CLP (Figure 5a). Similarly, wild-type mice treated with
190 the P2X7-receptor-antagonist A438079 also presented an increase in bacterial load
191 (Figure 5b). Administration of recombinant CD14 to *P2rx7*$^{-/-}$ mice before the CLP
192 procedure resulted in a significant reduction in bacterial load in the serum, peritoneal
193 lavage and liver (Figure 5c). Cytokine and chemokine levels reduced in the serum of
194 *P2rx7*$^{-/-}$ mice after CLP and treatment with recombinant CD14 (Figure 5d,e). These
195 results suggest that extracellular CD14 is an important element in the P2X7 receptor
196 secretome to control bacterial dissemination and cytokine production during sepsis.

197

198 **Release of P2X7-receptor-dependent CD14 during sepsis is important for survival**

199 We and others have found that *P2rx7*$^{-/-}$ mice present higher mortality during sepsis
200 (Csóka et al., 2015; Martínez-García et al., 2019), and here we also confirm that treating
201 wild-type mice with the pharmacological P2X7-receptor-antagonist A438079 before CLP
202 also increases the likelihood of mortality (Figure 6a). In line, CLP resulted in higher
203 decrease of mice body weight and poor well-being score on the supervision protocol in
204 *P2rx7*$^{-/-}$ mice and in wild-type mice treated with A438079 (Figure 6-supplement 1a,b).
205 To test if the deficiency in extracellular CD14 in *P2rx7*$^{-/-}$ mice during sepsis would be
206 detrimental for survival, we treated *P2rx7*$^{-/-}$ mice with recombinant CD14 before CLP
207 and found that mice survival was significantly increased (Figure 6b), as well as weight
208 loss was preserved (Figure 6-supplement 1a). This is in agreement with the reduction in
209 the bacterial load induced by recombinant CD14 treatment (Figure 5c). We next
210 evaluated organ damage as a direct cause of sepsis mortality and we found that the liver
211 of wild-type mice displayed an unstructured parenchyma and ballooning hepatocytes
212 after CLP (Figure 6c and Supplementary File 1-Table 2), which was aggravated in
213 *P2rx7*$^{-/-}$ mice or wild-type mice treated with A437089 and which further presented

214 prominent steatosis and dying hepatocytes (Figure 6c). Spleen and lung damage
215 induced by CLP in *P2rx7*$^{-/-}$ mice or wild-type mice treated with A438079 were also
216 exacerbated (Figure 6-supplement 1c and 2 and Supplementary File 1-Table 2). The
217 spleen exhibited a severe depletion of white pulp with the presence of apoptotic bodies
218 and congestion of red pulp (Figure 6-supplement 1c and 2), whereas the lungs showed
219 a marked leukocyte infiltration and intra-alveolar capillary hemorrhages with alveolar
220 thickening (Figure 6-supplement 1c and 2). Treating *P2rx7*$^{-/-}$ mice with recombinant
221 CD14 before CLP resulted in less pronounced damage in liver, spleen and lung (Figure
222 6d-supplement 3 and Supplementary File 1-Table 2). Altogether, our results demonstrate
223 that the P2X7 receptor controls the release of CD14 in extracellular vesicles, impairing
224 LPS signaling in myeloid cells and controlling bacteria and cytokine production during
225 sepsis, thus reducing tissue damage and improving survival.

226 **DISCUSSION**

227 Our study shows for first time that the cellular release of CD14 induced by the P2X7
228 receptor has two functional effects on the innate immune system: (*i*) it decreases CD14-
229 dependent pro-inflammatory signaling in macrophages, and (*ii*) it decrease bacterial
230 dissemination, improving survival during sepsis. In macrophages, the activation of the
231 P2X7 receptor controls many different responses, including the activation of the NLRP3
232 inflammasome or the unconventional release of different cellular proteins (de Torre-
233 Minguela et al., 2016; Di Virgilio et al., 2017). The release mechanism for the secretome
234 associated with P2X7-receptor activation is not characterize, but some are proteins
235 released mainly by inflammasome-dependent pyroptosis (de Torre-Minguela et al.,
236 2016). In this study we describe that the release of CD14 correlates with the extracellular
237 vesicle fraction, together with the tetraspanin CD9, rather than with the caspase-1
238 dependent pyroptotic soluble fraction. In fact, the release of CD14 was independent on
239 caspase-1 activity. Due to the heterogeneity of extracellular vesicle populations released
240 from cells and the fact that the P2X7 receptor has been associated with the release of
241 different extracellular vesicles such as microvesicles and exosomes (Kowal et al., 2016;
242 MacKenzie et al., 2001; Qu et al., 2009), our data supports that CD14 could be mainly a
243 component of exosomes because CD14 largely appears associated with the high speed
244 pellet containing “small” vesicles of ~160 nm. However, we could not rule out CD14
245 containing extracellular vesicles and exosomes may originate in the plasma membrane
246 because there is a net reduction in plasma-membrane-associated CD14 and the
247 presence of CD9 or IL-1β in this fraction has been correlated with both exosomes and
248 plasma membrane-derived “small” vesicles (Kowal et al., 2016; MacKenzie et al., 2001;
249 Qu et al., 2007). Furthermore, the inflammasome deficiency does not affect the release
250 of CD14, but it does decrease the amount of “small” extracellular vesicles after P2X7
251 receptor activation, this finding being in accordance with a previous study demonstrating
252 that NLRP3 impairs the release of exosomes from P2X7-receptor-activated dendritic

253 cells (Qu et al., 2009). Therefore, it remains difficult to determine the exact nature of the
254 extracellular vesicles containing CD14.

255 The release of CD14 occurred 5 min after stimulation in resting macrophages after brief
256 activation of the P2X7 receptor. Under these circumstances, the NLRP3 inflammasome
257 is not primed and therefore is not activated, thus protecting the cells from pyroptotic cell
258 death (Broz et al., 2020). However, it has been recently described that prolonged P2X7
259 receptor activation would lead to apoptosis in resting macrophages (Bidula et al., 2019).
260 The brief P2X7 receptor activation in resting macrophages with millimolar concentrations
261 of ATP used in this study did not compromise cell viability and may resemble
262 physiological conditions where ectonucleotidases provoke a fast ATP degradation in the
263 extracellular milieu (Eltzschig et al., 2012). Under these conditions, there is a reduction
264 in the subsequent production of pro-inflammatory cytokines after a smooth LPS
265 activation that requires CD14 to signal via the TLR4-MD2 complex (Pizzuto et al., 2018;
266 Ryu et al., 2017). This suggests that the release of CD14 from macrophages impairs
267 CD14 signaling, and probably also the translocation of TLR4 complex to endosomes,
268 thus impairing TRAM-TRIF-dependent pathways (Zanoni et al., 2013). However,
269 cytokine production was not affected when macrophages were treated with MPLA after
270 P2X7 receptor activation, because MLPA does not require CD14 to signal (Jiang et al.,
271 2005; Maeshima and Fernandez, 2013). The reduction in cytokine production upon LPS-
272 priming induced by initial P2X7 receptor activation in macrophages is additional to the
273 effect we have described on the inflammasome activation (Martínez-García et al., 2019),
274 because NLRP3 activation was affected when macrophages were primed using both
275 LPS and MLPA. All this suggests that brief P2X7 receptor activation before LPS priming
276 has a widespread inhibitory effect on the pro-inflammatory functions of the macrophage,
277 which includes reduced CD14 signaling and NLRP3 inflammasome activation. However,
278 it should be noted that the stimulation of P2X7 receptor after LPS priming enhance the
279 release of pro-inflammatory cytokines (de Torre-Minguela et al., 2016; Solle et al., 2001).

280 When P2X7 receptor is absent or pharmacologically blocked, the reduced levels of
281 circulating CD14 during sepsis is accompanied by an increase of cytokine release. Lower
282 levels of cytokines were restored by the addition of recombinant CD14. This strongly
283 suggests that the release of CD14 induced by P2X7 receptor during sepsis reduces the
284 induction of cytokine by bacterial LPS, being in line with the fact that a reduced amount
285 of CD14 at the plasma membrane impairs LPS and other PAMPs signaling (Akashi-
286 Takamura and Miyake, 2008; Baumann et al., 2010; Weber et al., 2012) and circulating
287 CD14 binds LPS and impair its signaling from plasma membrane receptors (Kitchens
288 and Thompson, 2005).

289 CD14 release has been described during infection due to proteinase dependent
290 shedding; however there is also a proteinase-independent CD14 release that is less well
291 understood (Wu et al., 2019). Our study demonstrates that the release of extracellular
292 vesicles induced by P2X7 receptor activation is a pathway contributing to the
293 extracellular pool of CD14. During sepsis, cell-free CD14 is present in serum and other
294 body fluids and has been proposed as a marker for septic patients (Bas et al., 2004;
295 Zhang et al., 2015), in fact the presence of CD14 in the blood has been validated by
296 different studies as a valuable prognostic capacity to predict mortality (Behnes et al.,
297 2014). CD14 increase in plasma during the first 24 h after sepsis initiation and remains
298 elevated at least during the first 8 days, conferring an exceptional long-term prognostic
299 value over acute phase proteins or IL-6 that quickly decrease after 3-8 days of sepsis
300 (Behnes et al., 2014; Martínez-García et al., 2019). This is similar to the CLP model
301 presented in this study, where while serum IL-6 concentration remains constant between
302 1 and 2 days of sepsis initiation, CD14 increased. Extracellular CD14 is required for host
303 defense and in particular for bacterial clearance (Fang et al., 2017; Knapp et al., 2006;
304 Sahay et al., 2018; Wieland et al., 2005), being necessary for phagocytosis of bacteria
305 (Grunwald et al., 1996; Lingnau et al., 2007; Schiff et al., 1997). Likewise, we found that
306 P2X7 receptor deficiency or its pharmacological inhibition reduces CD14 in peritoneal

307 lavage and serum when mice are subjected to a sepsis model. In these circumstances,
308 there is an increase in bacterial dissemination that was controlled by the exogenous
309 reconstitution of extracellular CD14. The decreased levels of CD14 in the infection foci
310 of our model, the peritoneum of P2X7 deficient mice, could be then the cause of the
311 increased to bacterial dissemination from peritoneum and infection of distant tissues and
312 organs, thus compromising animal viability. This is in agreement with a previous study
313 that found the P2X7 receptor to be important for bacterial clearance during sepsis (Csóka
314 et al., 2015).The dissemination of bacteria in the blood during sepsis exacerbates the
315 immune response and leads to life-threatening complications, such as organ failure and
316 ultimately death (Barratt-Due et al., 2017). *P2rx7* deficient mice present aggravated
317 damage to different organs and premature deaths during sepsis and the administration
318 of recombinant CD14 restores survival in the *P2rx7*$^{-/-}$genotype mice. This effect is similar
319 to wild-type mice, where the administration of CD14 increases survival (Haziot et al.,
320 1995). Therefore, P2X7 receptor-dependent release of CD14 seems to have a role in
321 bacterial infection restraint, and while we studied CD14 release from macrophages, there
322 are also reports indicating that non-hematopoietic cells such as epithelial or endothelial
323 cells that also express the P2X7 receptor could release CD14, thus also influencing
324 innate immune functions during infection (Jersmann, 2005) and in turn restoring
325 homeostatic conditions after sepsis (Zanoni et al., 2013).

326 In conclusion, we have identified the release of CD14 by extracellular vesicles as part of
327 the previously identified P2X7 receptor secretome of macrophages. The release of CD14
328 induced by the P2X7 receptor affects CD14 signaling in macrophages because the
329 activation by smooth LPS was affected and fewer pro-inflammatory cytokines were
330 produced. During sepsis, the elevation of CD14 levels in the serum and peritoneal
331 lavage, also depended on the P2X7 receptor, were important in controlling cytokine
332 secretion, restricting bacterial dissemination and organ damage, increasing overall
333 survival. Therefore, circulating CD14 is not only a marker for sepsis but also an important

334 component of the host's innate immune system because the P2X7 receptor releases it

335 in a regulated manner in order to control infection and increase survival during sepsis.

336 **MATERIALS & METHODS**

337 **Key resources table**

| Reagent type (species) or resource | Designation | Source or reference | Identifiers | Additional information |
|---|---|---|---|---|
| Strain, strain background (*S. minnesota*) | Monophosphoryl Lipid A (MPLA) | Invivogen | Cat#: tlrl-mpla | Cell culture: 1 µg/mL |
| Genetic reagent (*Mus musculus*, male) | P2RX7-deficient mice (*P2rx7*$^{-/-}$) | Jackson laboratories | B6.129P2-*P2rx7*$^{tm1Gab}$/J | *In vivo* mouse models and biological samples.<br><br>RRID: IMSR_JAX:005576 |
| Antibody | Anti-MMR (rat monoclonal, clone MR5D3) | Acris antibodies | Cat#:SM1857P | WB (1:1000),<br><br>RRID: AB_1611247 |
| Antibody | Anti-Cystatin B (rat monoclonal, clone 227818) | R&D | Cat#: MAB1409 | WB (1:1000),<br><br>RRID: AB_2086095 |
| Antibody | Anti-Cathepsin B (rat monoclonal, clone 173317) | R&D | Cat#: MAB965 | WB (1:1000),<br><br>RRID: AB_2086935 |
| Antibody | Anti-Peptidyl-prolyl cis-trans isomerase A (rabbit monoclonal) | Abcam | Cat#: ab41684 | WB (1:1000),<br><br>RRID: AB_879768 |

| | | | | |
|---|---|---|---|---|
| Sequence-based reagent | KiCqStart SYBR Green Primers | Sigma-Aldrich | *Tnfa* (NM_013693) *Il-6* (NM_031168) *Il1b* (NM_008361) | qRT-PCR |
| Peptide, recombinant protein | Human sCD14 recombinant protein | Preprotech | Cat#: 110-01 | *In vivo*: 10µg/g<br>RRID: AB_2877062 |
| Commercial assay, kit | ExoQuick-TC ULTRA EV isolation kit | System Biosciences (SBI) | Cat#: EQULTRA-20TC-1 | Extracellular vesicle isolation |
| Commercial assay, kit | Mouse CD14 DuoSet Elisa kit | R&D Systems | Cat#:DY982 | Detection of CD14 in biological fluids and culture supernatants.<br>RRID: AB_2877065 |
| Commercial assay, kit | Magnetic Luminex Assay | R&D Systems | Cat#: LXSAMSM-15 | Multiplex for mice serum |
| Chemical compound, drug | ATP | Sigma-Aldrich | A2383-5G | Cell culture: 3 mM<br>For FACS: 5 mM |
| Chemical compound, drug | A438079 | Tocris | Cat#: 2972 | Cell culture: 10-20 µM<br>*In vivo*: 100 µg/kg<br>For FACS: 10 µM |
| Software, algorithm | NTA 3.1 software | Nano Sight Technology | NS300 instrument | Nanoparticle tracking analysis,<br>RRID: SCR_014239 |

338

339 **Mice.** All experimental protocols for animal handling were refined and approved by the
340 Animal Health Service of the General Directorate of Fishing and Farming of the Council
341 of Murcia (*Servicio de Sanidad Animal, Dirección General de Ganadería y Pesca,*

342 *Consejería de Agricultura y Agua Región de Murcia,* referenceA1320140201). C57BL/6
343 mice (WT, wild-type, RRID: IMSR_JAX:000664) and P2X7 receptor-deficient mice in
344 C57BL/6 background (*P2rx7*$^{-/-}$; RRID: IMSR_JAX:005576) (Solle et al., 2001) were
345 obtained from the Jackson Laboratories. NLRP3-deficient (*Nlrp3*$^{-/-}$) (Martinon et al.,
346 2006) and Caspase-1/11 deficient (*Casp1/11*$^{-/-}$) (Kuida et al., 1995) in C57BL/6
347 background were a generous gift from I. Coullin. For all experiments, mice between 8-
348 10 weeks of age were used. Mice were bred in specific pathogen-free conditions with a
349 12:12 h light-dark cycle and used in accordance with the *Hospital Clínico Universitario*
350 *Virgen Arrixaca* animal experimentation guidelines, and Spanish national (Royal Decree
351 1201/2005 and Law 32/2007) and EU (86/609/EEC and 2010/63/EU) legislation.

352

353 **Cecal ligation and puncture**. The cecal ligation and puncture (CLP)-induced sepsis
354 procedure was performed in wild-type and *P2rx7*$^{-/-}$ mice as previously described
355 (Rittirsch et al., 2009). Briefly, a laparotomy was performed to isolate the cecum of mice
356 anesthetized with isoflurane (3–5% for induction and 1,5–2% for maintenance and
357 oxygen flow to 1 L/min). Approximately 2/3 of the cecum was ligated with a 6-0 silk suture
358 and punctured twice through-and-through with a 21 gauge needle. The abdominal wall
359 and incision were closed with 6-0 silk suture. Sham operated animals underwent
360 laparotomy without ligation or puncture of the cecum. Buprenorphine (0.3 mg/kg) was
361 administered intraperitoneally (i.p.) at the time of surgery and mice were monitored
362 continuously until recovery from anesthesia. 24 or 48 h after the procedure, the animals
363 were euthanized by $CO_2$ inhalation and peritoneal lavages and blood and tissue samples
364 were collected. In some experiments, *P2rx7*$^{-/-}$ mice received an i.p. injection of human
365 recombinant CD14 (10µg/g, Peprotech, RRID: AB_2877062) or vehicle (sterile
366 physiologic saline) 30 min prior to the CLP procedure. In some experiments, wild-type
367 mice were injected with A438079 (100µM/kg, i.p.) or vehicle 1 h prior to the CLP
368 procedure.

369

370 **Mouse sample collection.** Blood samples were obtained by thoracic aorta and were
371 centrifuged at 12,500*g*for 10 min. The recovered serum was stored at -80ºC until further
372 use. For collecting peritoneal lavage, the abdominal wall was exposed by opening the
373 skin; 4 ml of sterile saline were injected into the peritoneal cavity via a 25 gauge needle.
374 The abdomen was gently massaged for 1 min and the peritoneal fluid was recovered
375 through the needle and centrifuged at 433 *g* for 10 min to obtain a cell-free peritoneal
376 lavage. The supernatant was stored at -80ºC until further analysis. For tissue harvesting
377 the abdominal wall was exposed, the organs were removed using scissors and forceps
378 and were fixed and paraffin-embedded or stored at -80°C for future analysis.

379

380 **Quantification of bacterial colony forming units (CFU).** Fresh liver samples were
381 homogenized mechanically in sterile physiologic saline. Serum, peritoneal lavages and
382 tissue samples were diluted serially in sterile physiological saline and 100 μl of each
383 dilution was plated in Luria-Bertani agar and cultured on agar plates at 37ºC. After 24h
384 of incubation, the number of bacterial colonies (CFU) was counted in the various dilutions
385 and only used the dilutions where separate colonies were obtained. Bacterial load was
386 calculated by multiplying CFUs to the corresponding dilution and divided by the volume
387 inoculated to obtain the expressed CFU/ml of serum or peritoneal exudates or CFU/g of
388 liver.

389

390 **Histopathology**. Liver, spleen and lung tissues were fixed in 4% *p*-formaldehyde (PFA,
391 Sigma) for 24 h, processed, paraffin-embedded and sections stained with hematoxylin
392 and eosin using standard methods to evaluate damage. Slides were examined using a
393 Zeiss Axio Scope AX10 microscope with an AxioCamICC3 (Carl Zeiss).

394

395 **Differentiation and *in vitro* stimulation of macrophages.** Bone marrow derived
396 macrophages (BMDMs) were obtained from wild-type, *P2rx7*$^{-/-}$,*Nlrp3*$^{-/-}$ and *Casp1/11*$^{-/-}$
397 mice by differentiating bone marrow cells for 7 days in DMEM (Lonza) supplemented
398 with 25% of L929 medium, 15% fetal calf serum (FCS, Life Technologies), 100 U/ml
399 penicillin/streptomycin (Lonza), and 1% L-glutamine (Lonza) as described elsewhere
400 (Barberà-Cremades et al., 2012). Cells were primed with ultrapure *E. coli* LPS serotype
401 O55:B5 (10 ng/ml, Invivogen) or recombinant mouse IL-4 (20 ng/ml, BD Pharmingen,
402 RRID: AB_2868873) for 4 h. Cells were then washed three times with physiological buffer
403 before and then stimulated for 20 min with ATP (3 mM, Sigma-Aldrich) in E-total buffer
404 (147mMNaCl, 10mM HEPES, 13 mM glucose, 2mM $CaCl_2$, 1mM $MgCl_2$, and 2mMKCl,
405 pH 7.4). In other cases, cells were pretreated with ATP (3 mM) in the presence or
406 absence of the specific P2X7 receptor antagonist A438079 (Tocris, 10-20μM) in E-total
407 buffer and then washed and stimulated with LPS or 1 μg/ml of*S. Minnesota*
408 Monophosphoryl Lipid A (MPLA, Invivogen) for 4 h. Then cells were treated with 10 μM
409 of nigericin sodium salt (Sigma-Aldrich) for 30 min in E-total. In some experiments
410 BMDMs were incubated with 20 μg/ml of the blocking antibody anti-CD14 clone M14-23
411 (Biolegend) before LPS or MPLA were added. Supernatants were collected and clarified
412 at 14,000 *g* for 30 seconds at 4ºC to remove floating cells and stored at -80ºC until
413 cytokine determination. Cells were lysed immediately in lysis buffer (50 mM Tris-HCl pH
414 8.0, 150 mM NaCl, 2% Triton X-100) supplemented with 100 μl/ml of protease inhibitor
415 mixture (Sigma) for 30 min on ice and then cell debris was removed by centrifugation at
416 16,000 *g* for 15 min at 4°C.

417

418 **Extracellular vesicle isolation by ultracentrifugation.** Extracellular vesicles were
419 purified as previously described (Théry et al., 2006), diagram shown in Figure 1-

420 supplement 2c. Briefly, differentiated BMDMs in 150 $mm^2$ plates were washed with PBS
421 and incubated 24 h in medium with extracellular vesicle-depleted FBS. The cells were
422 primed with 10 ng/mL LPS, 20 ng/ml IL-4 or complete cell culture media alone for 4 h at
423 37°C, then washed three times with E-total buffer and incubated in the same buffer with
424 ATP 3 mM for 20 min. The collected medium was immediately transferred into a tube
425 containing Protease inhibitor mix (Sigma) on ice, and then followed by sequential
426 centrifugation at 4°C for 20 min at 2,000 *g*, (Sigma 3-18KS, rotor 11180&13190), 30 min
427 at 10,000 *g*, and 1 h at 100,000 *g* (Beckman Ultracentrifuge Optima L-80 XP, SW40
428 rotor). The supernatant of this last step was stored at -80ºC. The pellet from 100,000 *g*
429 was washed in 10 ml of PBS and centrifuged again for 1 h at 100,000 *g*. Finally,
430 extracellular vesicle fraction was collected in the pellet with 50 ml of PBS and stored at -
431 80ºC until use.

432

433 **Extracellular vesicles isolation by ExoQuick-TC ULTRA.** ExoQuick precipitation was
434 carried out following the manufacturer's instructions (System Biosciences), diagram
435 shown in Figure 1-supplement 2d. Briefly, 800 µl of cell culture supernatant or 2 ml or
436 peritoneal lavage was diluted to 5 ml in PBS and mixed with 1 ml of ExoQuick-TC solution
437 by inverting the tube several times. The sample was incubated overnight at 4°C then
438 centrifuged twice at 3,000*g*for 10 min to isolate extracellular vesicles. Later, extracellular
439 vesicles were centrifuged at 1,000 *g* for 30 seconds in order to purify them.

440

441 **Western blot.** Cells lysates, total cell-free supernatants, extracellular vesicle fraction and
442 extracellular vesicle-free supernatants were resolved in 4–12% precast Criterion
443 polyacrylamide gels (Biorad) and transferred to nitrocelulose membranes (Biorad) by
444 electroblotting as it is described in (de Torre-Minguela et al., 2016). Cell-free and
445 extracellular-free supernatants were precipitated overnight at -20°C with 6 volume of cold

446 acetone. Membranes were probed with different antibodies: anti-CD14 rat monoclonal
447 (rmC5-3, BD Pharmingen, RRID: AB_395020), anti-CD9 rabbit monoclonal (EPR2949,
448 ab92726, Abcam, RRID: AB_10561589), anti-MMR rat monoclonal (MR5D3, Acris
449 Antibodies, RRID: AB_1611247), anti-Cystatin B rat monoclonal (Clone #227818, R&D,
450 RRID: AB_2086095), anti-Cathepsin B rat monoclonal (Clone #173317, R&D, RRID:
451 AB_2086935), or anti-Peptidyl-prolyl cis-trans isomerase A rabbit polyclonal (ab41684,
452 Abcam, RRID: AB_879768).

453

454 **Nanoparticle Tracking Analysis.** After ultracentrifugation, 100K pellet was analyzed
455 with an NS300 nanoparticle tracking analysis (NTA) instrument, (NanoSight Technology)
456 to determine the vesicle size distributions and concentrations. Data was analyzed with
457 NTA 3.1 software (RRID: SCR_014239).

458

459 **Transmission electron microscopy (TEM).** Electron microscopy analysis was
460 performed as previously described (Théry et al., 2006) on pellets of purified extracellular
461 vesicle loaded on form var-carbon coated grids and fixed in 2% PFA. Grids were
462 observed at 80 kV with a JEM-1011 Transmission Electron Microscope (JEOL
463 Company). EV were counted for each preparation in 5 different random fields of TEM
464 pictures taken at 25,000x. The number of EV was then normalized to the number of cells
465 obtained in each treatment.

466

467 **Flow cytometry.** For membrane CD14 flow cytometry, BMDMs seeded in 24-well plates
468 were washed and incubated for 30 min at 37°C in E-total buffer supplemented with or
469 without 5 mM of ATP, in presence or absence of P2X7 receptor antagonist A438079 (10
470 μM). To stain surface CD14, cells were washed and incubated with mouse seroblock
471 FcR (BD biosciences) and then stained with anti-mouse CD14 (clone rmC5-3; 553738;

472 BD biosciences; RRID: AB_395020) for 30 min at 4ºC. Cells were washed again and
473 incubated with secondary Alexa Fluor 647 goat anti-rat IgG (H+L) (A21247; Invitrogen,
474 RRID: AB_141778) for an additional 30 min at 4ºC. Finally, cells were washed and fixed
475 with 4% PFA in PBS and then scrapped and aliquoted in flow cytometry tubes. For
476 human P2X7 flow cytometry, monocytes were determined from peripheral blood
477 mononuclear cells from non-septic and septic patients by $CD3^{-}$ $CD14^{+}$ selection, and
478 P2X7 receptor surface expression was determined using the monoclonal anti-P2X7 L4
479 clone (Buell et al., 1998; Martínez-García et al., 2019). All samples were subjected to
480 flow cytometry analysis using a BD FACSCanto flow cytometer (BD) and FACSDiva
481 software (BD, RRID: SCR_001456) by gating for BMDM cells based on FSC *versus* SSC
482 parameters.
483

484 **Quantitative reverse transcriptase–polymerase chain reaction (RT-PCR) analysis.**
485 BMDMs plated in 96-well plates, were stimulated as described above. Total RNA
486 extraction was performed using the RNAqueous Micro Kit (Invitrogen), followed by
487 reverse transcription using iScript cDNA Synthesis (Bio-Rad) with oligo-dT. The mix
488 SYBR Premix ExTaq (Takara) was used for quantitative PCR in iCycler My iQ
489 thermocycler (Bio-Rad). Specific primers were purchased from Sigma (KiCq Start SYBR
490 Green Primers). Only a single product was seen on melting curve analysis, and for each
491 primer set, the efficiency was > 95%. For the relative expression of mouse *Il6, Tnfa,* and
492 *Il1b*, their Ct was normalized to the housekeeping gene *Gapdh* using the $2^{-\Delta Ct}$ method.

493

494 **Human clinical samples**. The samples and data from patients included in this study
495 were provided by the *Biobanco en Red de la Región de Murcia* (PT13/0010/0018), which
496 is integrated into the Spanish National Biobanks Network (B.000859) and approved by
497 the clinical ethics committee of the Clinical University Hospital *Virgen de la Arrixaca*

498 (reference numbers PI13/00174, 2019-9-4-HCUVA, 2019-12-15-HCUVA and 2019-12-
499 14-HCUVA). All study procedures were conducted in accordance with the declaration of
500 Helsinki. Whole peripheral blood samples were collected after receiving written informed
501 consent from intraabdominal sepsis patients (*n* = 9, Supplementary File 1-Table 1) at the
502 Surgical Critical Unit from the Clinical University Hospital *Virgen de la Arrixaca*. The
503 blood samples were obtained from septic individuals within 24 h of the diagnosis of
504 sepsis. The inclusion criteria for septic patients were patients diagnosed with intra-
505 abdominal origin sepsis confirmed by exploratory laparotomy, with at least two diagnostic
506 criteria for sepsis (fever or hypothermia; heart rate >90 beats per minute; tachypnea,
507 leukocytosis, or leukopenia) and multiple organ dysfunction defined as physiological
508 dysfunction in two or more organs or organ systems (Singer et al., 2016). We also
509 recruited non-septic volunteers and after they had signed their informed consent
510 agreement whole peripheral blood samples were collected (*n* = 10). Sera was isolated
511 and stored at -80ºC until use.

512

513 **ELISA and multiplex assay.** Individual culture cell-free supernatants were collected and
514 clarified by centrifugation. The concentration of IL-6 (RRID: AB_2877063), TNF-α (RRID:
515 AB_2877064), IL-1β (RRID: AB_2574946) and CD14 (RRID: AB_2877065) was tested
516 by ELISA following the manufacturer's instructions (R&D Systems and Thermo Fisher).
517 Mice serum and peritoneal lavages were collected and the concentration of IL-6 and
518 CD14 was also tested by ELISA (R&D Systems). Results were read in a Synergy Mx
519 (BioTek) plate reader. Multiplexing in mice serum for MCSF, CRP, RAGE, Resistin,
520 VEGF, MIP-1α, MIP-1β, MIP-2, CCL2, CCL5, IL-1α, IL-5 and IL-10was performed using
521 the Luminex color-coded superparamagnetic beads array from R&D Systems following
522 the manufacturer indications, and the results were analyzed in a Bio-Rad Bio-Plex
523 analyzer.

524

525 **Statistical analysis.** Statistical analyses were performed using GraphPad Prism 7
526 (Graph-Pad Software, Inc, RRID: SCR_002798). For two-group comparisons, the Mann-
527 Whitney test was used and Kaplan-Meier survival curves were plotted and the log-rank
528 test was undertaken to determine the statistical significance. The $\chi^2$ test was used to
529 determine whether there was a significant difference between different clinical variables
530 among groups of septic patients, except for age, where a one-way ANOVA test was
531 used. For mouse *in vivo* data and before statistical analysis, possible outliers were
532 identified with the robust regression followed by outlier identification method with Q=1%
533 and were eliminated from the analysis and representation. All data are shown as mean
534 values and error bars represent standard error from the number of independent assays
535 indicated in the figure legend. $p$ value is indicated as *$p$ <0.05; **$p$ <0.01; ***$p$<0.001;
536 ****$p$ <0.0001; $p$ >0.05 not significant (*ns*).

537

538 **Acknowledgments**

539 We would like to thank M.C. Baños and A.I. Gómez (IMIB-Arrixaca, Murcia, Spain) for
540 technical assistance with molecular and cellular biology and the members of Dr
541 Pelegrin's laboratory for comments and suggestions, especially to Dr. M. Pizzuto for
542 critical reading the manuscript. We would also like to acknowledge the patients and
543 volunteers who enrolled in this study, the BioBank Biobanco en Red de la Región de
544 Murcia (PT13/0010/0018), which is integrated into the Spanish National Biobanks
545 Network (B.000859) for its collaboration and the SPF-animal house from IMIB-Arrixaca
546 for mice colony maintenance. **Funding**: This work was supported by the Ministerio de
547 Economía, Industria y Competitividad (grant SAF2017-88276-R), Fundación Séneca
548 (grants 20859/PI/18 and 21081/PDC/19), and the European Research Council (ERC-
549 2013-CoG grant 614578 and ERC-2019-PoC grant 899636).

550

551 **Declaration of interests**

552 The authors declare no competing interests.

553

554 **REFERENCES**


555 Akashi-Takamura S, Miyake K. 2008. TLR accessory molecules. *Curr Opin Immunol*
556 **20**:420–425. doi:10.1016/j.coi.2008.07.001

557 Barberà-Cremades M, Baroja-Mazo A, Gomez AI, Machado F, Di Virgilio F, Pelegrín P.
558 2012. P2X7 receptor-stimulation causes fever *via* PGE2 and IL-1β release.
559 *FASEB J* **26**:2951–2962. doi:10.1096/fj.12-205765

560 Barratt-Due A, Pischke SE, Nilsson PH, Espevik T, Mollnes TE. 2017. Dual inhibition of
561 complement and Toll-like receptors as a novel approach to treat inflammatory
562 diseases—C3 or C5 emerge together with CD14 as promising targets. *J Leukoc*
563 *Biol* **101**:193–204. doi:10.1189/jlb.3vmr0316-132r

564 Bas S, Gauthier BR, Spenato U, Stingelin S, Gabay C, Bas S, Gauthier BR, Gauthier
565 BR, Spenato U, Spenato U, Stingelin S, Stingelin S, Gabay C. 2004. CD14 Is an
566 Acute-Phase Protein. *J Immunol* **172**:4470–4479.
567 doi:10.4049/jimmunol.172.7.4470

568 Baumann CL, Aspalter IM, Sharif O, Pichlmair A, Blüml S, Grebien F, Bruckner M,
569 Pasierbek P, Aumayr K, Planyavsky M, Bennett KL, Colinge J, Knapp S, Superti-
570 Furga G. 2010. CD14 is a coreceptor of Toll-like receptors 7 and 9. *J Exp Med*
571 **207**:2689–2701. doi:10.1084/jem.20101111

572 Behnes M, Bertsch T, Lepiorz D, Lang S, Trinkmann F, Brueckmann M, Borggrefe M,
573 Hoffmann U. 2014. Diagnostic and prognostic utility of soluble CD 14 subtype
574 (presepsin) for severe sepsis and septic shock during the first week of intensive
575 care treatment. *Crit Care* **18**:507. doi:10.1186/s13054-014-0507-z

576 Bidula S, Dhuna K, Helliwell R, Stokes L. 2019. Positive allosteric modulation of P2X7
577 promotes apoptotic cell death over lytic cell death responses in macrophages. *Cell*
578 *Death Dis* **10**:882. doi:10.1038/s41419-019-2110-3

579 Broz P, Pelegrín P, Shao F. 2020. The gasdermins, a protein family executing cell
580 death and inflammation. *Nat Rev Immunol* **20**:143–157. doi:10.1038/s41577-019-
581 0228-2

582 Buell G, Chessell IP, Michel AD, Collo G, Salazzo M, Herren S, Gretener D, Grahames
583 C, Kaur R, Kosco-Vilbois MH, Humphrey PP. 1998. Blockade of human P2X7
584 receptor function with a monoclonal antibody. *Blood* **92**:3521–3528.

585 Csóka B, Németh ZH, Töro G, Idzko M, Zech A, Koscsó B, Spolarics Z, Antonioli L,
586 Cseri K, Erdélyi K, Pacher P, Haskó G. 2015. Extracellular ATP protects against
587 sepsis through macrophage P2X7 purinergic receptors by enhancing intracellular
588 bacterial killing. *FASEB J* **29**:3626–3637.

589 de Torre-Minguela C, Barberà-cremades M, Gomez AI, Martin-Sanchez F, Pelegrin P,
590 Barbera-Cremades M, Gomez AI, Martin-Sanchez F, Pelegrin P, Torre-minguela
591 C De, Barberà-cremades M, Gómez AI, Martín-Sánchez F, de Torre-Minguela C,
592 Barberà-cremades M, Gómez AI, Martín-Sánchez F, Pelegrín P. 2016.
593 Macrophage activation and polarization modify P2X7 receptor secretome
594 influencing the inflammatory process. *Sci Rep* **6**:22586. doi:10.1038/srep22586

595 Di Virgilio F, Dal Ben D, Sarti AC, Giuliani AL, Falzoni S. 2017. The P2X7 Receptor in
596 Infection and Inflammation. *Immunity* **47**:15–31. doi:10.1016/j.immuni.2017.06.020

597 Eltzschig HK, Sitkovsky M V, Robson SC. 2012. Purinergic Signaling during
598 Inflammation. *N Engl J Med* **367**:2322–2333. doi:10.1056/NEJMra1205750

599 Fang K, Kwon M-H, Lahoud MH, Qin K, Ma S, Li H, Wu M, Sun Y, Fu M, Guo Z, Zhu H,
600 Gong F, Lei P, Shen G. 2017. GRP78 Impairs Production of Lipopolysaccharide-
601 Induced Cytokines by Interaction with CD14. *Front Immunol* **8**:579.
602 doi:10.3389/fimmu.2017.00579

603 Grunwald U, Fan X, Jack RS, Workalemahu G, Kallies A, Stelter F, Schutt C. 1996.

604 Monocytes can phagocytose Gram-negative bacteria by a CD14-dependent
605 mechanism. *J Immunol* **157**:4119–4125.

606 Haziot A, Rong GW, Lin XY, Silver J, Goyert SM. 1995. Recombinant soluble CD14
607 prevents mortality in mice treated with endotoxin (lipopolysaccharide). *J Immunol*
608 **154**:6529–32.

609 Jersmann HP. 2005. Time to abandon dogma: CD14 is expressed by non-myeloid
610 lineage cells. *Immunol Cell Biol* **83**:462–467. doi:10.1111/j.1440-
611 1711.2005.01370.x

612 Jiang Z, Georgel P, Du X, Shamel L, Sovath S, Mudd S, Huber M, Kalis C, Keck S,
613 Galanos C, Freudenberg M, Beutler B. 2005. CD14 is required for MyD88-
614 independent LPS signaling. *Nat Immunol* **6**:565–570. doi:10.1038/ni1207

615 Kitchens RL, Thompson PA. 2005. Modulatory effects of sCD14 and LBP on LPS-host
616 cell interactions. *J Endotoxin Res* **11**:225–229. doi:10.1179/096805105X46565

617 Knapp S, Wieland CW, Florquin S, Pantophlet R, Dijkshoorn L, Tshimbalanga N, Akira
618 S, Van Der Poll T. 2006. Differential roles of CD14 and Toll-like receptors 4 and 2
619 in murine Acinetobacter pneumonia. *Am J Respir Crit Care Med* **173**:122–129.
620 doi:10.1164/rccm.200505-730OC

621 Kowal J, Arras G, Colombo M, Jouve M, Morath JP, Primdal-Bengtson B, Dingli F,
622 Loew D, Tkach M, Théry C. 2016. Proteomic comparison defines novel markers to
623 characterize heterogeneous populations of extracellular vesicle subtypes. *Proc*
624 *Natl Acad Sci* **113**:E968–E977. doi:10.1073/pnas.1521230113

625 Kuida K, Lippke J, Ku G, Harding M, Livingston D, Su M, Flavell R. 1995. Altered
626 cytokine export and apoptosis in mice deficient in interleukin-1 beta converting
627 enzyme. *Science (80- )* **267**:2000–2003. doi:10.1126/science.7535475

628 Lévêque M, Simonin-Le Jeune K, Jouneau S, Moulis S, Desrues B, Belleguic C,

629 Brinchault G, Le Trionnaire S, Gangneux J-P, Dimanche-Boitrel M-T, Martin-
630 Chouly C. 2017. Soluble CD14 acts as a DAMP in human macrophages: origin
631 and involvement in inflammatory cytokine/chemokine production. *FASEB J*
632 **31**:1891–1902. doi:10.1096/fj.201600772R

633 Lingnau M, Höflich C, Volk H-D, Sabat R, Döcke W-D. 2007. Interleukin-10 enhances
634 the CD14-dependent phagocytosis of bacteria and apoptotic cells by human
635 monocytes. *Hum Immunol* **68**:730–738. doi:10.1016/j.humimm.2007.06.004

636 MacKenzie A, Wilson HL, Kiss-Toth E, Dower SK, North RA, Surprenant A. 2001.
637 Rapid secretion of interleukin-1beta by microvesicle shedding. *Immunity* **15**:825–
638 835.

639 Maeshima N, Fernandez RC. 2013. Recognition of lipid A variants by the TLR4-MD-2
640 receptor complex. *Front Cell Infect Microbiol*. doi:10.3389/fcimb.2013.00003

641 Martínez-García JJ, Martínez-Banaclocha H, Angosto-Bazarra D, de Torre-Minguela C,
642 Baroja-Mazo A, Alarcón-Vila C, Martínez-Alarcón L, Amores-Iniesta J, Martín-
643 Sánchez F, Ercole GA, Martínez CM, González-Lisorge A, Fernández-Pacheco J,
644 Martínez-Gil P, Adriouch S, Koch-Nolte F, Luján J, Acosta-Villegas F, Parrilla P,
645 García-Palenciano C, Pelegrin P. 2019. P2X7 receptor induces mitochondrial
646 failure in monocytes and compromises NLRP3 inflammasome activation during
647 sepsis. *Nat Commun* **10**:2711. doi:10.1038/s41467-019-10626-x

648 Martinon F, Pétrilli V, Mayor A, Tardivel A, Tschopp J. 2006. Gout-associated uric acid
649 crystals activate the NALP3 inflammasome. *Nature* **440**:237–241.

650 McGaraughty S, Chu KL, Namovic MT, Donnelly-Roberts DL, Harris RR, Zhang X-F,
651 Shieh CC, Wismer CT, Zhu CZ, Gauvin DM, Fabiyi AC, Honore P, Gregg RJ, Kort
652 ME, Nelson DW, Carroll WA, Marsh K, Faltynek CR, Jarvis MF. 2007. P2X7-
653 related modulation of pathological nociception in rats. *Neuroscience* **146**:1817–

654 1828.

655 Pellegatti P, Raffaghello L, Bianchi G, Piccardi F, Pistoia V, Di Virgilio F. 2008.
656 Increased level of extracellular ATP at tumor sites: in vivo imaging with plasma
657 membrane luciferase. *PLoS One* **3**:e2599. doi:10.1371/journal.pone.0002599

658 Pizzuto M, Bigey P, Lachagès A-M, Hoffmann C, Ruysschaert J-M, Escriou V, Lonez
659 C. 2018. Cationic lipids as one-component vaccine adjuvants: A promising
660 alternative to alum. *J Control Release* **287**:67–77.
661 doi:10.1016/j.jconrel.2018.08.020

662 Qu Y, Franchi L, Nunez G, Dubyak GR. 2007. Nonclassical IL-1β Secretion Stimulated
663 by P2X7 Receptors Is Dependent on Inflammasome Activation and Correlated
664 with Exosome Release in Murine Macrophages. *J Immunol* **179**:1913–1925.
665 doi:10.4049/jimmunol.179.3.1913

666 Qu Y, Qu Y, Ramachandra L, Ramachandra L, Mohr S, Mohr S, Franchi L, Franchi L,
667 Harding C V, Harding C V, Nunez G, Nunez G, Dubyak GR, Dubyak GR. 2009.
668 P2X7 Receptor-Stimulated Secretion of MHC Class II-Containing Exosomes
669 Requires the ASC/NLRP3 Inflammasome but Is Independent of Caspase-1. *J*
670 *Immunol* **182**:5052–5062. doi:10.4049/jimmunol.0802968

671 Rittirsch D, Huber-Lang MS, Flierl MA, Ward PA. 2009. Immunodesign of experimental
672 sepsis by cecal ligation and puncture. *Nat Protoc* **4**:31–6.
673 doi:10.1038/nprot.2008.214

674 Ryu JK, Kim SJ, Rah SH, Kang JI, Jung HE, Lee D, Lee HK, Lee JO, Park BS, Yoon
675 TY, Kim HM. 2017. Reconstruction of LPS Transfer Cascade Reveals Structural
676 Determinants within LBP, CD14, and TLR4-MD2 for Efficient LPS Recognition and
677 Transfer. *Immunity* **46**:38–50. doi:10.1016/j.immuni.2016.11.007

678 Sahay B, Bashant K, Nelson NLJ, Patsey RL, Gadila SK, Boohaker R, Verma A, Strle

679 K, Sellati TJ. 2018. Induction of Interleukin 10 by Borrelia burgdorferi Is Regulated
680 by the Action of CD14-Dependent p38 Mitogen-Activated Protein Kinase and
681 cAMP-Mediated Chromatin Remodeling. doi:10.1128/IAI.00781-17

682 Schiff DE, Kline L, Soldau K, Lee JD, Pugin J, Tobias PS, Ulevitch RJ. 1997.
683 Phagocytosis of gram-negative bacteria by a unique CD14-dependent
684 mechanism. *J Leukoc Biol* **62**:786–94. doi:10.1002/jlb.62.6.786

685 Setoguchi M, Nasu N, Yoshida S, Higuchi Y, Akizuki S, Yamamoto S. 1989. Mouse
686 and human CD14 (myeloid cell-specific leucine-rich glycoprotein) primary
687 structure deduced from cDNA clones. *Biochim Biophys Acta - Gene Struct Expr*
688 **1008**:213–222. doi:10.1016/0167-4781(80)90012-3

689 Singer M, Deutschman CS, Seymour CW, Shankar-Hari M, Annane D, Bauer M,
690 Bellomo R, Bernard GR, Chiche J-D, Coopersmith CM, Hotchkiss RS, Levy MM,
691 Marshall JC, Martin GS, Opal SM, Rubenfeld GD, van der Poll T, Vincent J-L,
692 Angus DC. 2016. The Third International Consensus Definitions for Sepsis and
693 Septic Shock (Sepsis-3). *JAMA* **315**:801. doi:10.1001/jama.2016.0287

694 Solle M, Labasi J, Perregaux DG, Stam E, Petrushova N, Koller BH, Griffiths RJ, Gabel
695 CA. 2001. Altered cytokine production in mice lacking P2X(7) receptors. *J Biol*
696 *Chem* **276**:125–32. doi:10.1074/jbc.M006781200

697 Théry C, Amigorena S, Raposo G, Clayton A. 2006. Isolation and Characterization of
698 Exosomes from Cell Culture Supernatants and Biological Fluids. *Curr Protoc Cell*
699 *Biol* **30**:3.22.1-3.22.29. doi:10.1002/0471143030.cb0322s30

700 Weber C, Müller C, Podszuweit A, Montino C, Vollmer J, Forsbach A. 2012. Toll-like
701 receptor (TLR) 3 immune modulation by unformulated small interfering RNA or
702 DNA and the role of CD14 (in TLR-mediated effects). *Immunology* **136**:64–77.
703 doi:10.1111/j.1365-2567.2012.03559.x

704 Wieland CW, Florquin S, Maris NA, Hoebe K, Beutler B, Takeda K, Akira S, van der
705 Poll T. 2005. The MyD88-Dependent, but Not the MyD88-Independent, Pathway
706 of TLR4 Signaling Is Important in Clearing Nontypeable Haemophilus influenzae
707 from the Mouse Lung . *J Immunol* **175**:6042–6049.
708 doi:10.4049/jimmunol.175.9.6042

709 Wu Z, Zhang Z, Lei Z, Lei P. 2019. CD14: Biology and role in the pathogenesis of
710 disease. *Cytokine Growth Factor Rev*. doi:10.1016/j.cytogfr.2019.06.003

711 Zanoni I, Granucci F, Gekara N, Bengoechea JA. 2013. Role of CD14 in host
712 protection against infections and in metabolism regulation.
713 doi:10.3389/fcimb.2013.00032

714 Zhang J, Hu Z-D, Song J, Shao J. 2015. Diagnostic Value of Presepsin for Sepsis.
715 *Medicine (Baltimore)* **94**:e2158. doi:10.1097/MD.0000000000002158

716

717 **FIGURE LEGENDS**

718 **Figure 1. P2X7 receptor stimulation induces the release of extracellular vesicles**
719 **containing CD14.** (**a**) Immunoblot for CD14 and CD9 in cell lysate (CL), cell-free
720 supernatant (Sup) and supernatant fractions (100K pellet and 100K supernatant)
721 obtained from extracellular vesicle (EV) isolation from BMDMs treated for 4h with LPS
722 (10 ng/ml) and then stimulated or not for 20 min with ATP (3 mM); representative of *n*=3
723 experiments. (**b**) Quantification of extracellular CD14 by ELISA in Sup, EV isolated with
724 the Exo-Quick kit and flow-through fraction obtained in cell-free supernatants from
725 BMDM treated as in (a), but before ATP application cells were treated for 10 min with
726 A438079 (20 μM) as indicated (left) or from EV isolated with the Exo-Quick in
727 supernatants from *P2rx7*$^{-/-}$ macrophages (right); each dot represents an independent
728 experiment (*n*= 4 to 8). (**c**) Immunoblot for CD14 and CD9 in Sup, 100K pellet and 100K
729 supernatant from BMDM cell-free supernatants treated as in (a), but after the first step
730 of EV isolation, Sup was treated with 2% of Triton X-100; representative of *n*= 3
731 independent experiments. (**d**) Immunoblot for CD14 and CD9 in Sup, 100K pellet and
732 100K supernatant in cell-free supernatants from BMDM unprimed or primed for 4h with
733 LPS (10 ng/ml) or IL-4 (20 ng/ml) and then treated with ATP as in (a); representative of
734 *n*= 3 experiments. (**e**) Quantification of EV released from BMDM treated as in (d), left
735 panel; each dot represents an independent experiment (*n*= 3 to 5); Normalized number
736 of EV to the number of cells obtained in each treatment is shown. Representative
737 transmission electron microscopy image obtained from the 100K pellet, right panel. (**f**)
738 Immunoblot for CD14 and CD9 in 100K pellet obtained from cell-free supernatants of
739 C57BL/6 (wild-type), *Nlrp3*$^{-/-}$ or *Casp1/11*$^{-/-}$ BMDM treated as in (a), representative of *n*=
740 3 independent experiments. (**g**) Quantification of EV in cell-free supernatants of C57BL/6
741 (wild-type), *Nlrp3*$^{-/-}$ or *Casp1/11*$^{-/-}$ BMDM treated as in (a); each dot represents an
742 independent experiment (*n*= 3 to 5); Normalized number of EV to the number of cells
743 obtained in each treatment is shown. **(h)** Quantification of CD14 mean fluorescence

744 intensity (MFI) in BDMD treated as in (b); each dot represents an independent
745 experiment (*n*= 6). **p*<0.05, ***p*<0.01, ****p*<0.001, Mann-Whitney test. For a,c,d,f
746 numbers on the right of the blots correspond to the molecular weight in kDa.
747
748 **Figure 1-supplement 1. (a)** Nanoparticle tracking analysis of extracellular vesicles
749 isolated from BMDM cell-free supernatant primed for 4 h with LPS (10 ng/ml) and then
750 stimulated during 20 min with ATP (3 mM); *n*= 3. **(b)** Immunoblot for macrophage
751 mannose receptor 1 (MMR), peptidyl-prolyl cis-trans isomerase A (PPIase), cathepsin B
752 (CathpB), cystatin B (CstB) and CD9 (left panel) or ELISA for IL-1b (right panel) in cell-
753 free supernatant (Sup) and fractions (100K pellet and 100K supernatant) obtained from
754 extracellular vesicles isolated from BMDM cell-free supernatant primed for 4 h with LPS
755 (10 ng/ml) and then stimulated or not during 20 min with ATP (3 mM); results are
756 representative from *n*= 2 independent experiments (left panel), or n= 4 to 8 independent
757 experiments (right panel); **p*< 0.05, ****p*< 0.001, Mann-Whitney test. **(c)** Immunoblot for
758 CD14 and CD9 in cell-free supernatant (Sup) and fractions (100K pellet and 100K
759 supernatant) obtained from extracellular vesicles isolated from BMDM cell-free
760 supernatant treated for 4 h with LPS (10 ng/ml) and then stimulated or not at indicated
761 times with ATP (3 mM); representative of *n*= 3 independent experiments. For b,c
762 numbers on the right of the blots correspond to the molecular weight in kDa.
763
764 **Figure 1-supplement 2.** (**a**) Representative transmission electron microscopy images
765 obtained from extracellular vesicle fraction isolated from cell-free supernatants of BMDM
766 untreated (resting) or primed for 4 h with LPS (10 ng/ml) or IL-4 (20 ng/ml) and then
767 stimulated during 20 min with ATP (3 mM). Representative images from *n*≥ 3
768 independent experiments. (**b**) Representative transmission electron microscopy images
769 obtained from 100K pellet fraction obtained from cell-free supernatant of *Casp1/11*$^{-/-}$ and
770 *Nlrp3*$^{-/-}$ BMDM primed for 4 h with LPS (10 ng/ml) and then stimulated during 20 min
771 with ATP (3 mM). Representative images of *n*= 3 independent experiments. (**c**) Diagram

772 for extracellular vesicle isolation protocol based on differential centrifugation. Speed,
773 duration and temperature of each centrifugation step are indicated. Pellets are discarded
774 after first two centrifugations and the supernatant is kept for the next step. In the last
775 100,000 x*g* centrifugation, 100K pellet fraction is obtained. (**d**) Diagram for extracellular
776 vesicle isolation protocol based on Exo-Quick kit.

777

778 **Figure 2. P2X7 receptor stimulation impairs LPS-mediated signalling.** (**a**)
779 Expression of *Il6* and *Tnfa* genes analysed by qPCR in C57BL/6 (wild-type) or *P2rx7*$^{-/-}$
780 BMDM treated or not for 10 min with A438079 (10 μM), then incubated for 30 min with
781 ATP (5 mM), then washed and finally primed for 4 h with LPS (10 ng/ml). (**b**) IL-6 and
782 TNF-α concentration in cell-free supernatants from C57BL/6 (wild-type) or *P2rx7*$^{-/-}$
783 BMDM treated as in (a). (**c,d**) Expression of *Il6* and *Tnfa* genes analysed by qPCR (**c**)
784 and ELISA for IL-6 and TNF-α in cell-free supernatants (**d**) from C57BL/6 (wild-type) or
785 *P2rx7*$^{-/-}$ BMDM treated as in (a) but finally stimulated for 4 h with MPLA (1 μg/ml) instead
786 of LPS. (**e**) Expression of *Il1b* gene analysed by qPCR from BMDM treated as in (a) and
787 (c). (**f**) IL-1β concentration in cell-free supernatants from BMDM treated as in (e) and
788 after LPS or MPLA stimulation, cells were incubated for 30 min with nigericin (10 μM).
789 Each dot represents a single independent experiment; data are represented as mean ±
790 SEM; $n$= 4 to 6 single experiments; *$p$< 0.05; **$p$< 0.01; *ns*, no significant difference ($p$>
791 0.05); Mann–Whitney test.

792

793 **Figure 2-supplement 1.** (**a**) Expression of *Il6* and *Tnfa* genes analysed by qPCR from
794 BMDM treated for 10 min with a blocking αCD14 antibody (clone M14-23, 20 μg/mL,
795 4ºC), and then cells were incubated for 4 h with LPS (10 ng/mL) or MPLA (1 μg/mL) at
796 37ºC. (**b**) Release of IL-6 and TNF-α from BMDMs treated as in (a). Each dot represents
797 a single independent experiment; mean ± standard error is represented in all panels; $n$=

798 4–5 independent experiments; *$p$< 0.05; **$p$< 0.01; *ns*, no significant difference ($p$ >
799 0.05); Mann–Whitney test.

800

801 **Figure 3. P2X7 receptor controls CD14 in extracellular vesicles during sepsis.** (**a**)
802 Blood plasma concentration of CD14 (left) and quantification of P2X7 receptor mean
803 fluorescence intensity (MFI) in monocytes (right) from non-septic donors and intra-
804 abdominal origin septic patients within the first 24 h of admission to the surgical unit.
805 Each dot represents a donor or septic individual, $n$= 10. (**b**) CD14 concentration in the
806 serum and peritoneal lavage of C57BL/6 (wild-type) and *P2rx7*$^{-/-}$ mice collected 24 and
807 48 h after CLP measured by ELISA. (**c**) CD14 concentration in the serum and peritoneal
808 lavage of C57BL/6 (wild-type) mice collected 24 h after CLP, treated or not with A438079
809 (100 μM/kg) 1 h before CLP. (**d**) CD14 concentration in extracellular vesicles (E.V.)
810 isolated from the peritoneal lavage of C57BL/6 (wild-type) and *P2rx7*$^{-/-}$ mice collected
811 48 h after CLP. For b–d, each dot represents a single mouse; data are represented as
812 mean ± SEM; *$p$<0.05; **$p$<0.01; ***$p$<0.0001; Mann-Whitney test**.**

813

814 **Figure 4. The deficiency or blocking of P2X7 receptor increases cytokine**
815 **production during sepsis.** (**a**) ELISA of IL-6 in the serum of C57BL/6 (wild-type) and
816 *P2rx7*$^{-/-}$ mice collected 24 and 48 h after CLP; each dot represents a single mouse; data
817 are represented as mean ± SEM; *$p$<0.05; Mann-Whitney test. (**b,c**) Heatmaps for the
818 concentrations of different cytokines, chemokines and acute phase proteins as indicated
819 in the serum of C57BL/6 (wild-type) and *P2rx7*$^{-/-}$ mice (**b**) or C57BL/6 treated with
820 A438074 (100 μM/kg) (**c**) collected 24 h after CLP. For (b,c) C57BL/6 sham $n$= 5 (b) and
821 $n$= 4 (c); *P2rx7*$^{-/-}$ sham $n$= 5; sham+A438079 $n$= 3; C57BL/6 CLP $n$= 8 (b) and $n$= 8 (c);
822 *P2rx7*$^{-/-}$ CLP $n$= 9; and C57BL/6 CLP+A438079 $n$= 6.

823

824 **Figure 5. Extracellular CD14 limits bacterial dissemination and cytokine**
825 **production during sepsis caused by P2X7 receptor deficiency.** (**a**) Bacterial load in
826 serum, peritoneal lavage and liver homogenates from C57BL/6 (wild-type) and *P2rx7*$^{-/-}$
827 mice collected 24 and 48 h after CLP. (**b**) Bacterial load in serum, peritoneal lavage and
828 liver homogenates from C57BL/6 (wild-type) mice treated with A438074 (100 μM/kg) and
829 collected 24 h after CLP. (**c**) Bacterial load in serum, peritoneal lavage and liver from
830 *P2rx7*$^{-/-}$ mice treated with recombinant CD14 (rCD14, 10 μg/g) 30 min before CLP and
831 collected 24 h after CLP. (**d**) ELISA for IL-6 in serum and peritoneal lavage samples from
832 *P2rx7*$^{-/-}$ mice collected 24 h after CLP with or without treatment with recombinant CD14
833 (rCD14, 10 μg/g) 30 min before CLP; each dot represents a single mouse and data are
834 represented as mean ± SEM. (**e**) Heatmaps for the concentrations of different cytokines,
835 chemokines and acute phase proteins as indicated in the serum of *P2rx7*$^{-/-}$mice treated
836 with rCD14 as in (d) collected 24 and 48 h after CLP. For a-d panels, each dot represents
837 a single mouse and data are represented as mean ± SEM; **p*<0.05; ***p*<0.01;
838 ****p*<0.001; *****p*<0.0001; Mann-Whitney test.

839

840 **Figure 6. Release of P2X7-receptor-dependent CD14 during sepsis is important for**
841 **survival.** (**a**) Kaplan-Meier analysis of C57BL/6 (wild-type) mice survival after sham
842 operation or CLP, a group of mice were treated with A438074 (100 μM/kg) before CLP.
843 Sham groups *n*= 6 each; CLP *n*= 14 and CLP+A438079 *n*= 10. (**b**) Kaplan-Meier analysis
844 of C57BL/6 (wild-type) and *P2rx7*$^{-/-}$ mice survival after sham operation or CLP. A group
845 of *P2rx7*$^{-/-}$ mice were treated with recombinant CD14 (rCD14, 10 μg/g) 30 min before
846 CLP. Sham groups *n*= 4 each; CLP *n*= 14, CLP *P2rx7*$^{-/-}$*n*= 9; and rCD14+CLP *P2rx7*$^{-/-}$*n*=
847 9. (**c,d**) Representative images of hematoxylin and eosin-stained liver sections 24 and
848 48 h after CLP of mouse groups described in (a,b); scale bar, 50 μm. CLP 24 h *n*= 9;
849 rCD14+CLP 24 h *n*= 7; CLP 48 h *n*= 4, rCD14+CLP 48 h *n*= 3. **p*<0.05; ***p*<0.01;

850 ****$p$<0.0001; *ns*, no significant difference ($p$> 0.05); Mann-Whitney test for e and Log-
851 rank (Mantel-Cox) test for a, b.

852

853 **Figure 6-supplement 1.** (**a**) Normalized body weight (weight at different times/weight at
854 the beginning, time 0: $g_t/g_0$) after sham operation or CLP for wild-type mice, wild-type
855 treated with A438079, *P2rx7*$^{-/-}$ mice, *P2rx7*$^{-/-}$ mice with rCD14 treatment; data are
856 represented as mean ± SEM of $n$= 6 animals per group, except $n$= 4 for the wild-type
857 sham group treated with A438079. (**b**) Monitorization score of $n$= 5 mice per group.
858 Animals were scored from the beginning of the study following individual values for: spiky
859 hair, weight loss, ocular discharge, bending posture, ataxia, trembling, hypothermia,
860 cyanosis, auto-mutilation, aggressive/comatose behaviour and stool type. When the
861 score was between 4 and 10, the animal was supervised every hour. (**c**) Representative
862 images of hematoxylin and eosin-stained liver, spleen and lung sections from C57BL/6
863 (wild-type) and *P2rx7*$^{-/-}$ mice 24 and 48 h after CLP. Scale bar 50 μm; images
864 representative of $n$= 6 independent mice.

865

866 **Figure 6-supplement 2.** Representative images of hematoxylin and eosin-stained liver,
867 spleen and lung sections obtained 24 h after CLP from C57BL/6 (wild-type) mice treated
868 with A438079 (100 μM/kg) 1 h before CLP. Scale bar 50 μm; images representative of
869 $n$= 6 independent mice.

870

871 **Figure 6-supplement 3.** Representative images of hematoxylin and eosin-stained liver,
872 spleen and lung sections obtained 24 h after CLP from *P2rx7*$^{-/-}$ mice treated with
873 recombinant CD14 (rCD14, 100 μg/g) 30 min before CLP. Scale bar 50 μm; images
874 representative of $n$= 6 independent mice.

875

876 **Supplementary File 1**. **Table1.** Demographics and clinical features of enrolled healthy
877 volunteers and patients with intra-abdominal sepsis. **Table 2**. Histopathology scoring
878 (average of *n*= 3 animals/group).

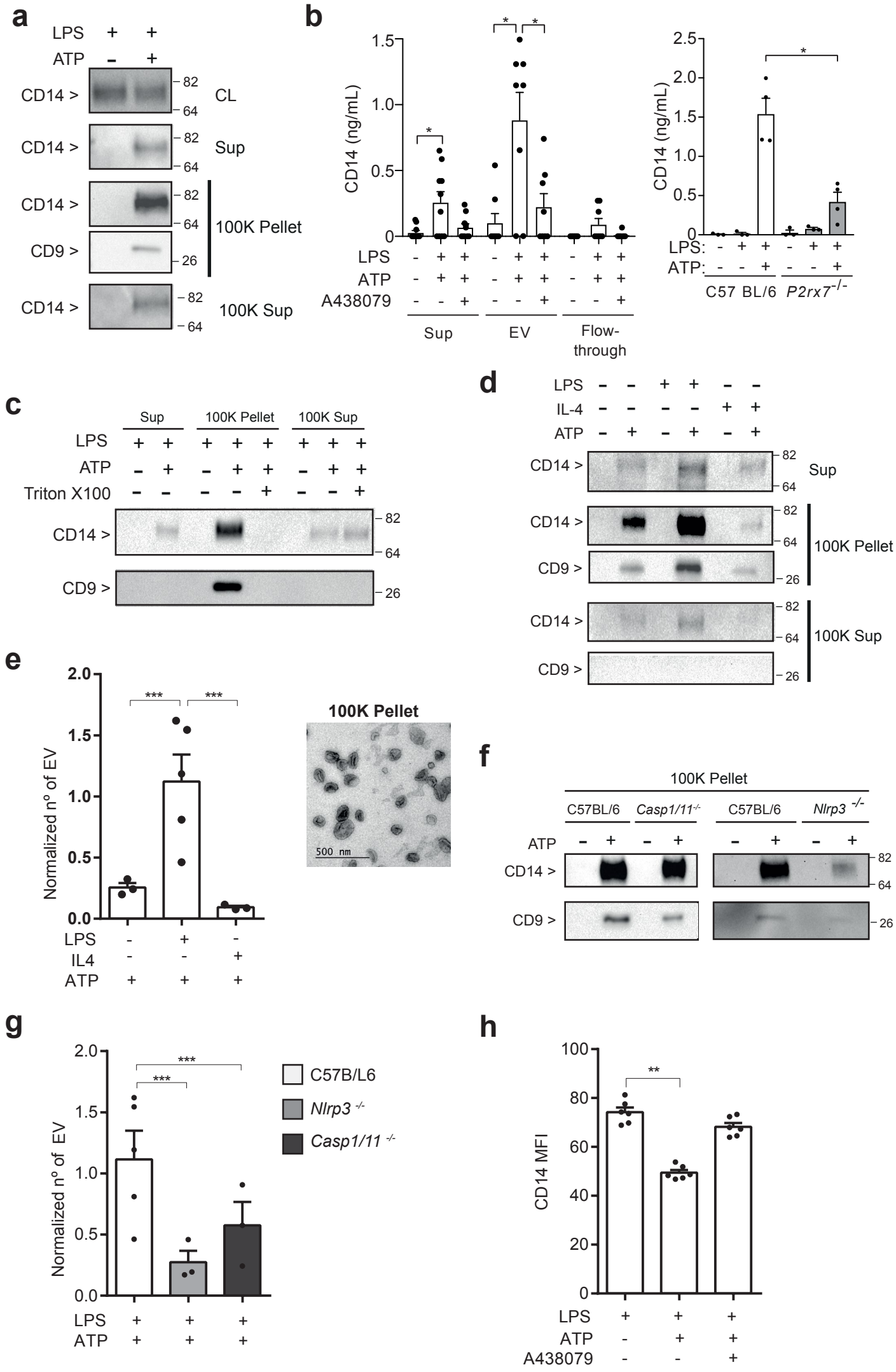
a
LPS + +
ATP - +
CD14 >
CD9 >
82
64
26
CL
Sup
100K Pellet
100K Sup
b
CD14 (ng/mL)
LPS
ATP
A438079
Sup
EV
Flow-through
C57 BL/6
P2rx7-/-
c
Sup
100K Pellet
100K Sup
Triton X100
d
IL-4
e
Normalized nº of EV
100K Pellet
500 nm
f
C57BL/6
Casp1/11-/-
Nlrp3 -/-
g
C57B/L6
Nlrp3 -/-
Casp1/11 -/-
h
CD14 MFI

**a**

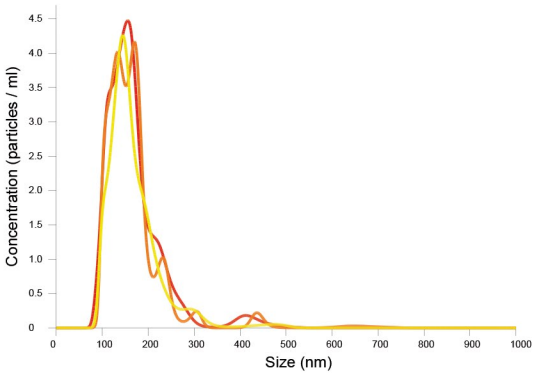


**Results**

Stats: Merged Data

| | |
|---|---|
| Mean: | 167.4 nm |
| Mode: | 143.8 nm |
| SD: | 64.6 nm |
| D10: | 109.0 nm |
| D50: | 153.5 nm |
| D90: | 230.8 nm |

Stats: Mean +/- Standard Error

| | |
|---|---|
| Mean: | 167.3 +/- 0.4 nm |
| Mode: | 156.9 +/- 7.4 nm |
| SD: | 64.2 +/- 3.8 nm |
| D10: | 109.2 +/- 0.9 nm |
| D50: | 153.5 +/- 0.5 nm |
| D90: | 230.5 +/- 2.0 nm |
| Concentration: | 4.08e+010 +/- 2.36e+009 particles/ml |
| | 51.7 +/- 3.0 particles/frame |
| | 53.3 +/- 2.8 centres/frame |

**b**

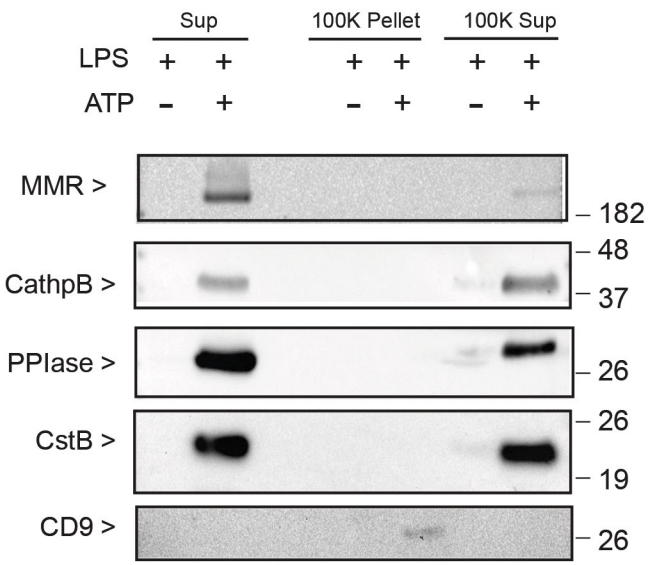


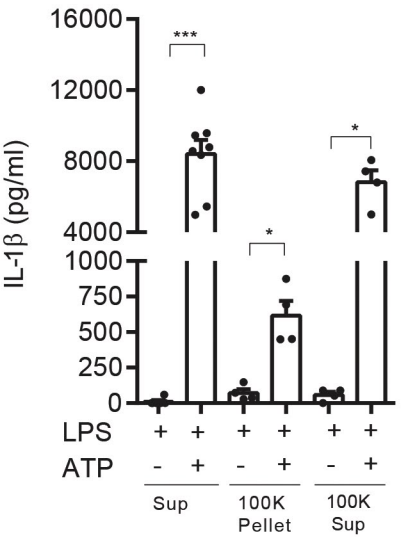


**c**

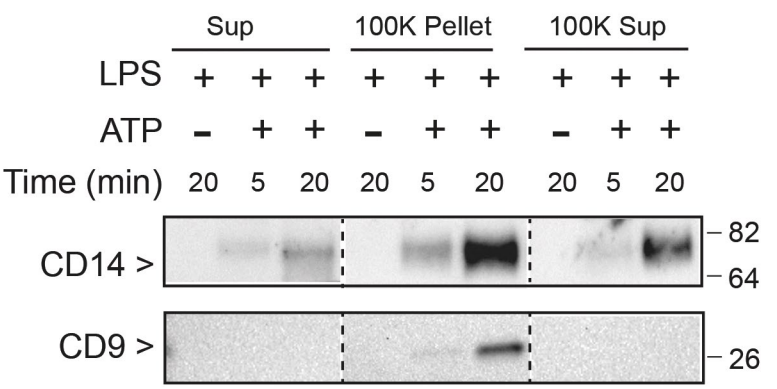

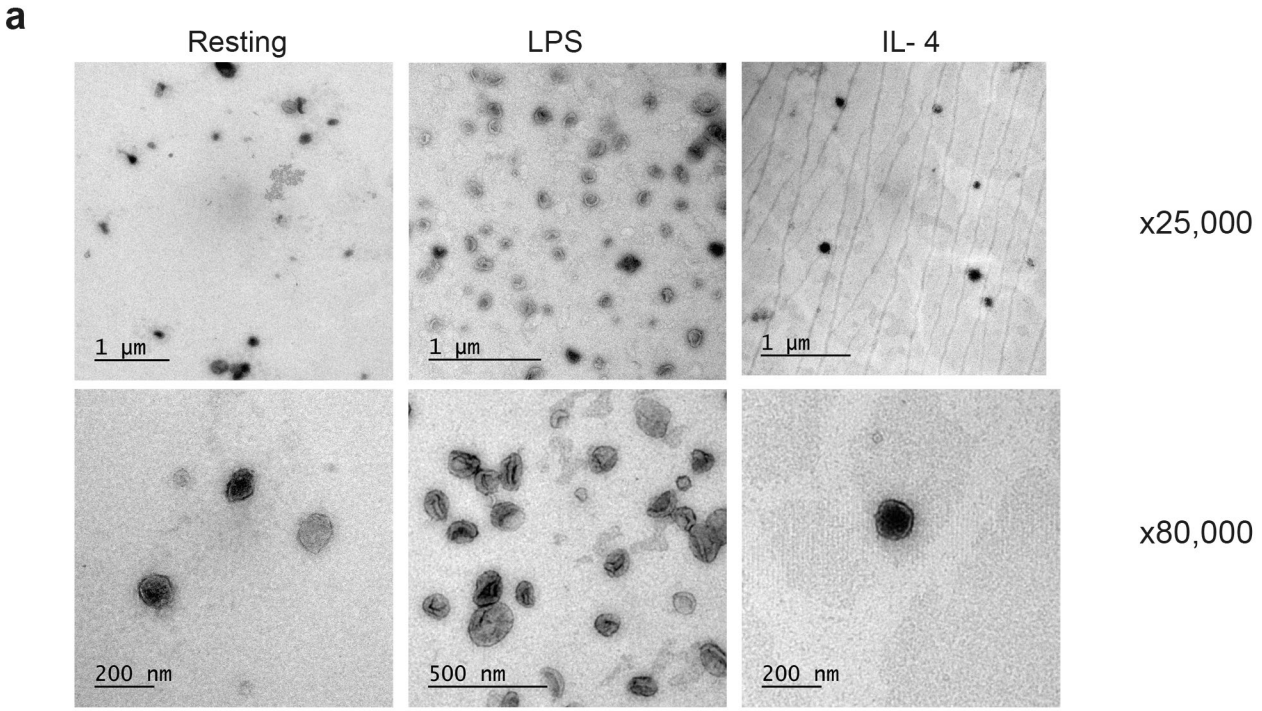
a
Resting
LPS
IL- 4
x25,000
x80,000
1 µm
1 µm
1 µm
200 nm
500 nm
200 nm

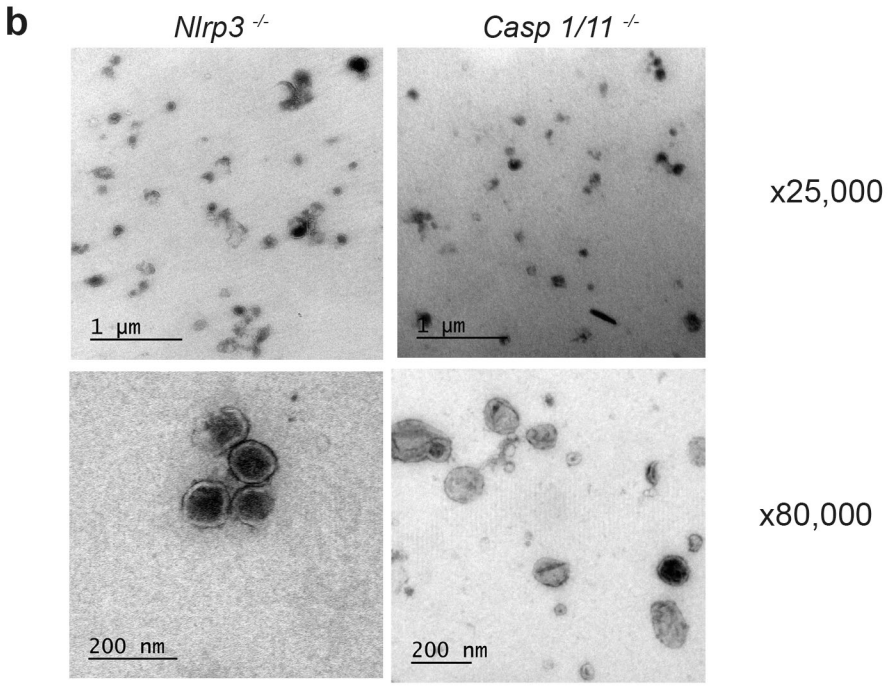
b
Nlrp3 -/-
Casp 1/11 -/-
x25,000
x80,000
1 µm
1 µm
200 nm
200 nm

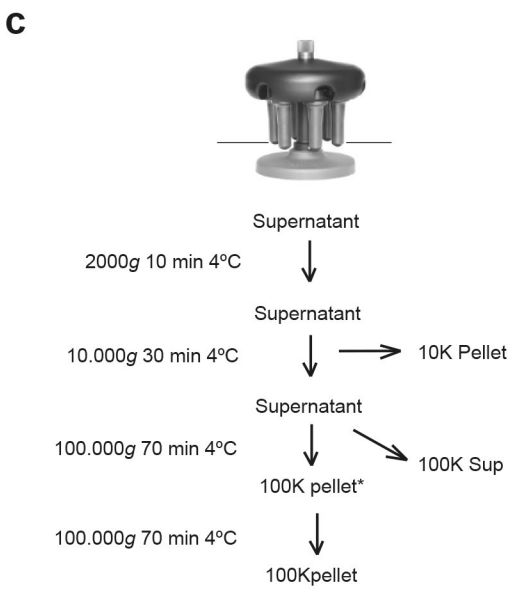
c
Supernatant
2000g 10 min 4ºC
Supernatant
10.000g 30 min 4ºC
10K Pellet
Supernatant
100.000g 70 min 4ºC
100K Sup
100K pellet*
100.000g 70 min 4ºC
100Kpellet

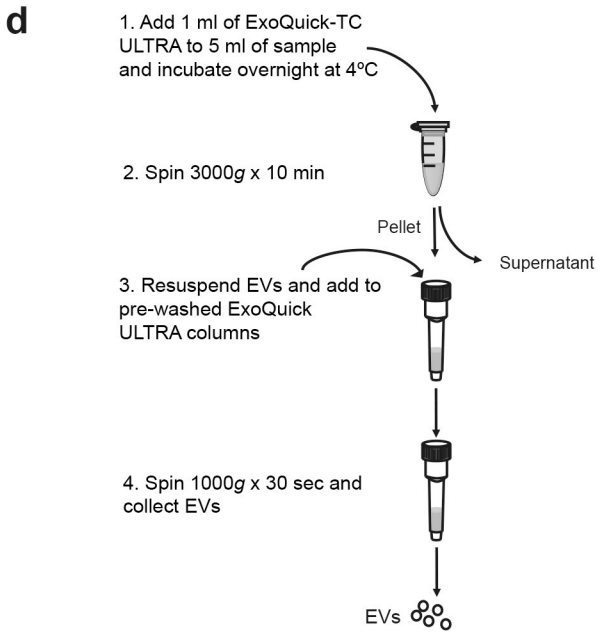
d
1. Add 1 ml of ExoQuick-TC ULTRA to 5 ml of sample and incubate overnight at 4ºC
2. Spin 3000g x 10 min
Pellet
Supernatant
3. Resuspend EVs and add to pre-washed ExoQuick ULTRA columns
4. Spin 1000g x 30 sec and collect EVs
EVs

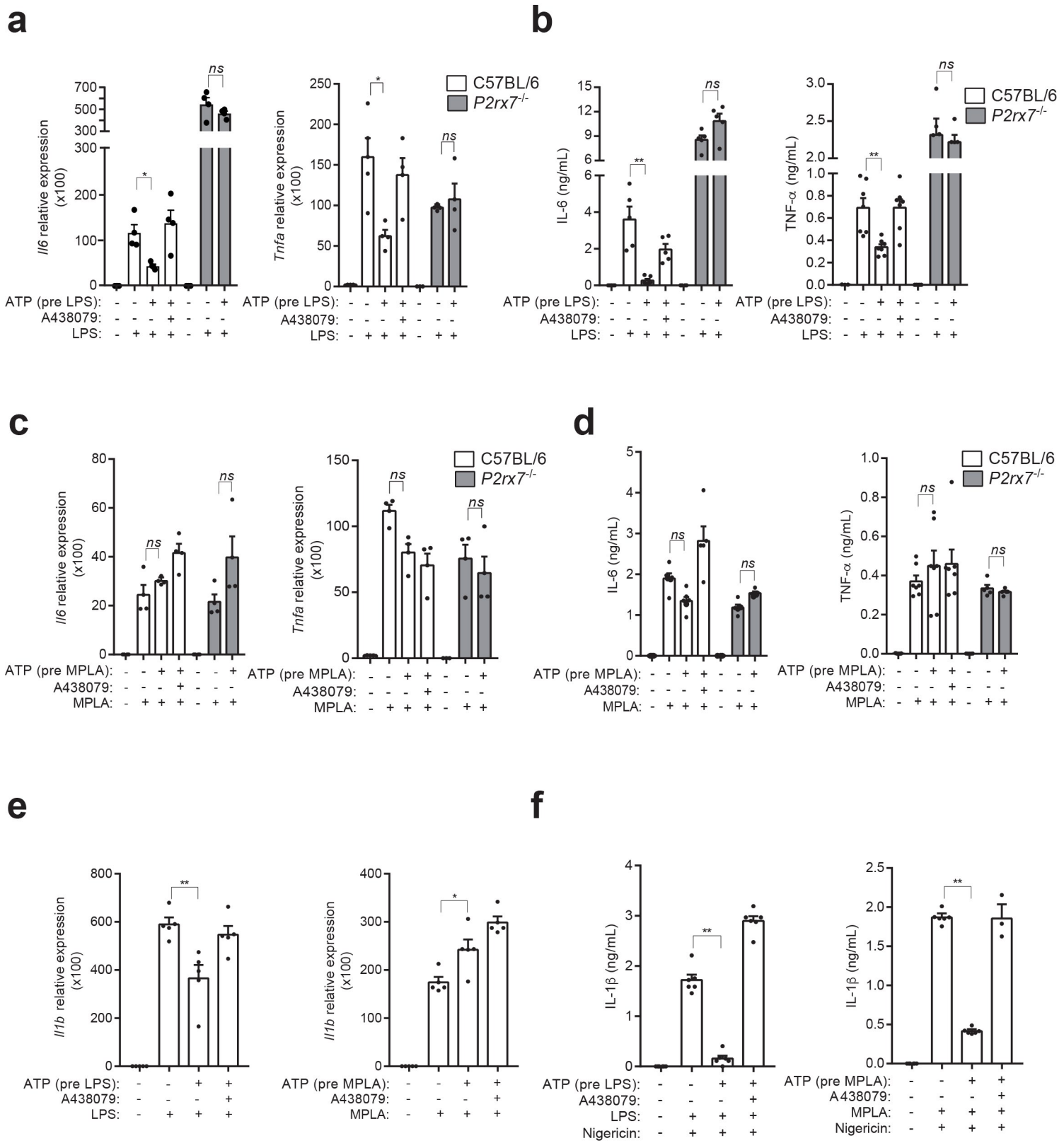
a
b
c
d
e
f
C57BL/6
P2rx7-/-
Il6 relative expression (x100)
Tnfa relative expression (x100)
IL-6 (ng/mL)
TNF-α (ng/mL)
Il1b relative expression (x100)
IL-1β (ng/mL)
ATP (pre LPS):
A438079:
LPS:
ATP (pre MPLA):
MPLA:
Nigericin:
ns
*
**

**a**

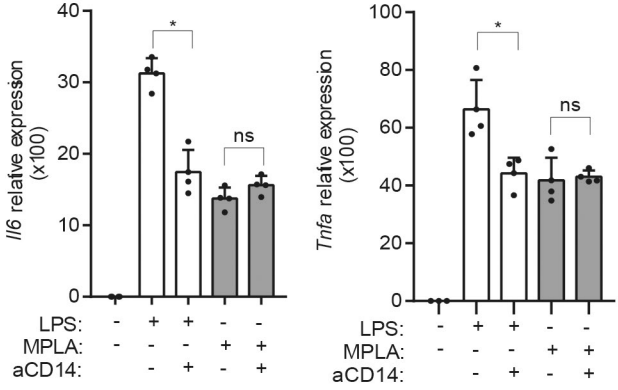
Il6 relative expression (x100)
40
30
20
10
0
*
ns
LPS: - + + - -
MPLA: - - - + +
aCD14: - + - +
Tnfa relative expression (x100)
100
80
60
40
20
0
*
ns
LPS: - + + - -
MPLA: - - - + +
aCD14: - + - +

**b**

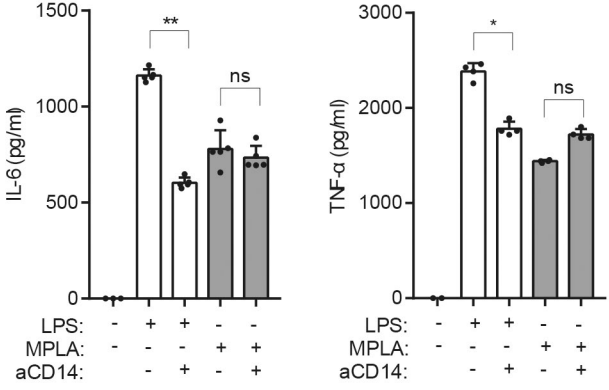
IL-6 (pg/ml)
1500
1000
500
0
**
ns
LPS: - + + - -
MPLA: - - - + +
aCD14: - + - +
TNF-α (pg/ml)
3000
2000
1000
0
*
ns
LPS: - + + - -
MPLA: - - - + +
aCD14: - + - +

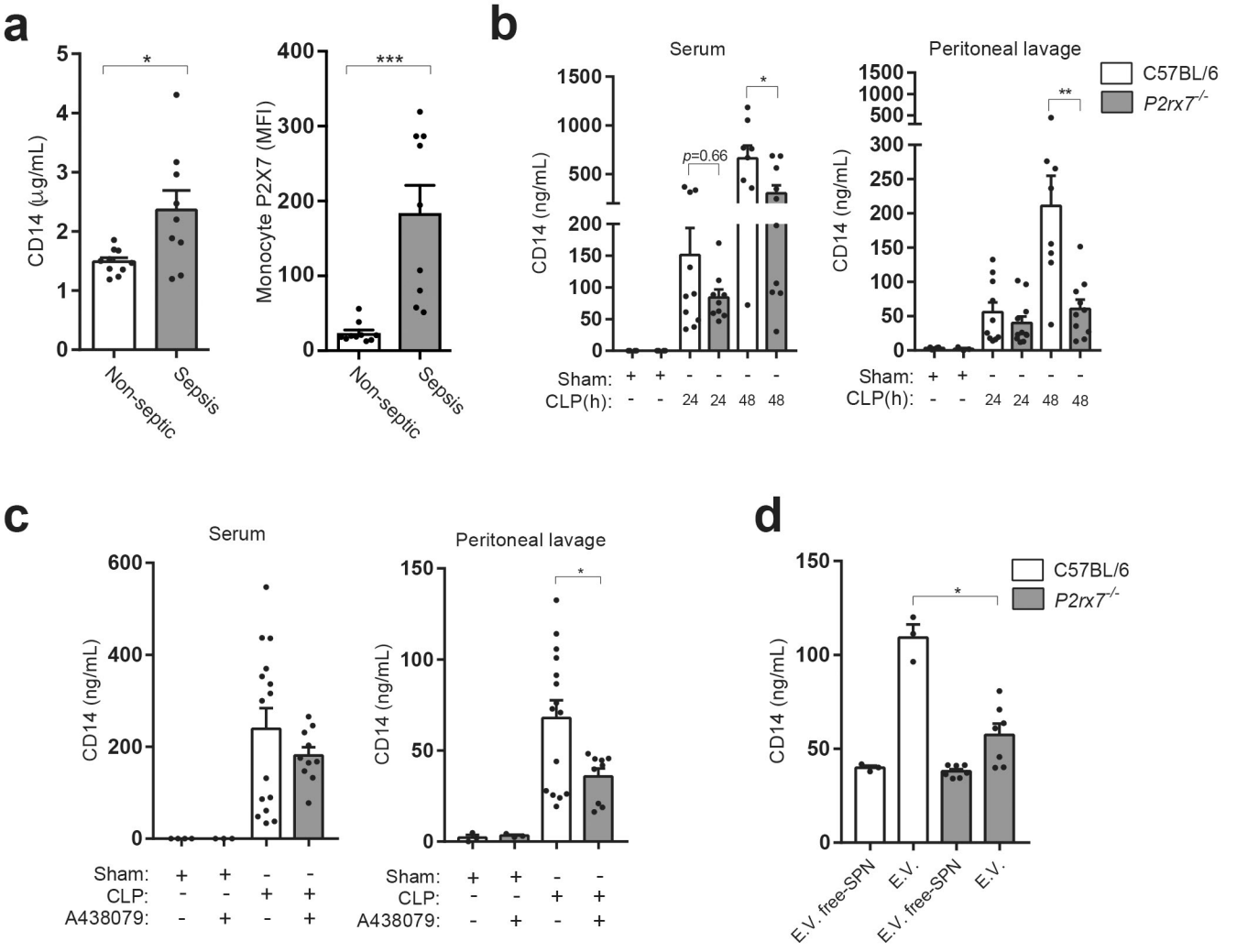
a
CD14 (µg/mL)
Non-septic
Sepsis
Monocyte P2X7 (MFI)
b
Serum
Peritoneal lavage
CD14 (ng/mL)
p=0.66
C57BL/6
P2rx7-/-
Sham:
CLP(h):
c
Serum
Peritoneal lavage
CD14 (ng/mL)
Sham:
CLP:
A438079:
d
CD14 (ng/mL)
C57BL/6
P2rx7-/-
E.V. free-SPN
E.V.

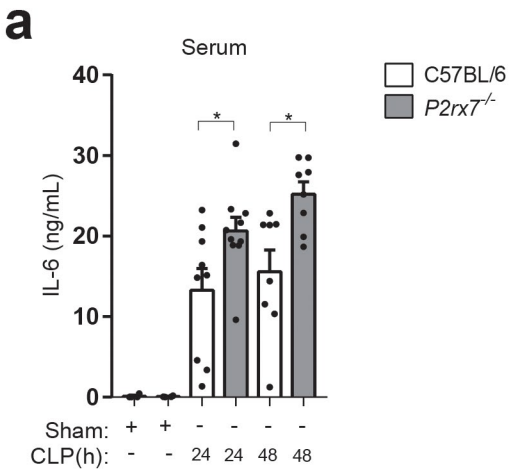
a
Serum
C57BL/6
P2rx7-/-
IL-6 (ng/mL)
40
30
20
10
0
*
*
Sham: + + - - - -
CLP(h): - - 24 24 48 48

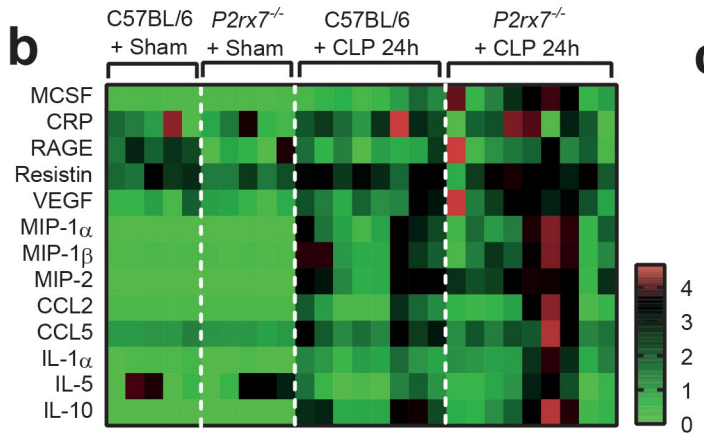
b
C57BL/6 + Sham
P2rx7-/- + Sham
C57BL/6 + CLP 24h
P2rx7-/- + CLP 24h
MCSF
CRP
RAGE
Resistin
VEGF
MIP-1α
MIP-1β
MIP-2
CCL2
CCL5
IL-1α
IL-5
IL-10
4
3
2
1
0

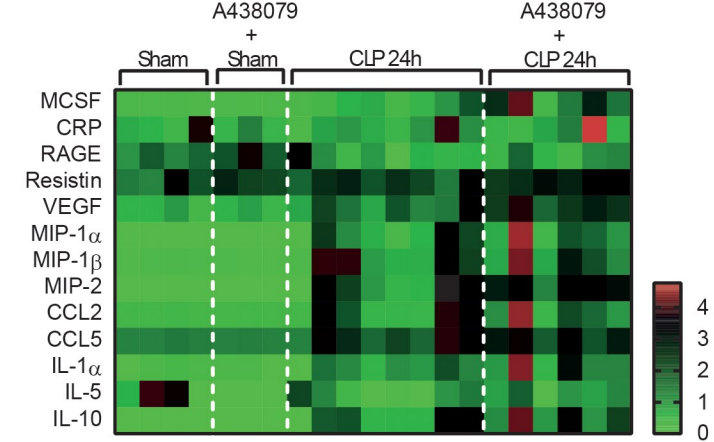
c
Sham
A438079 + Sham
CLP 24h
A438079 + CLP 24h
MCSF
CRP
RAGE
Resistin
VEGF
MIP-1α
MIP-1β
MIP-2
CCL2
CCL5
IL-1α
IL-5
IL-10
4
3
2
1
0

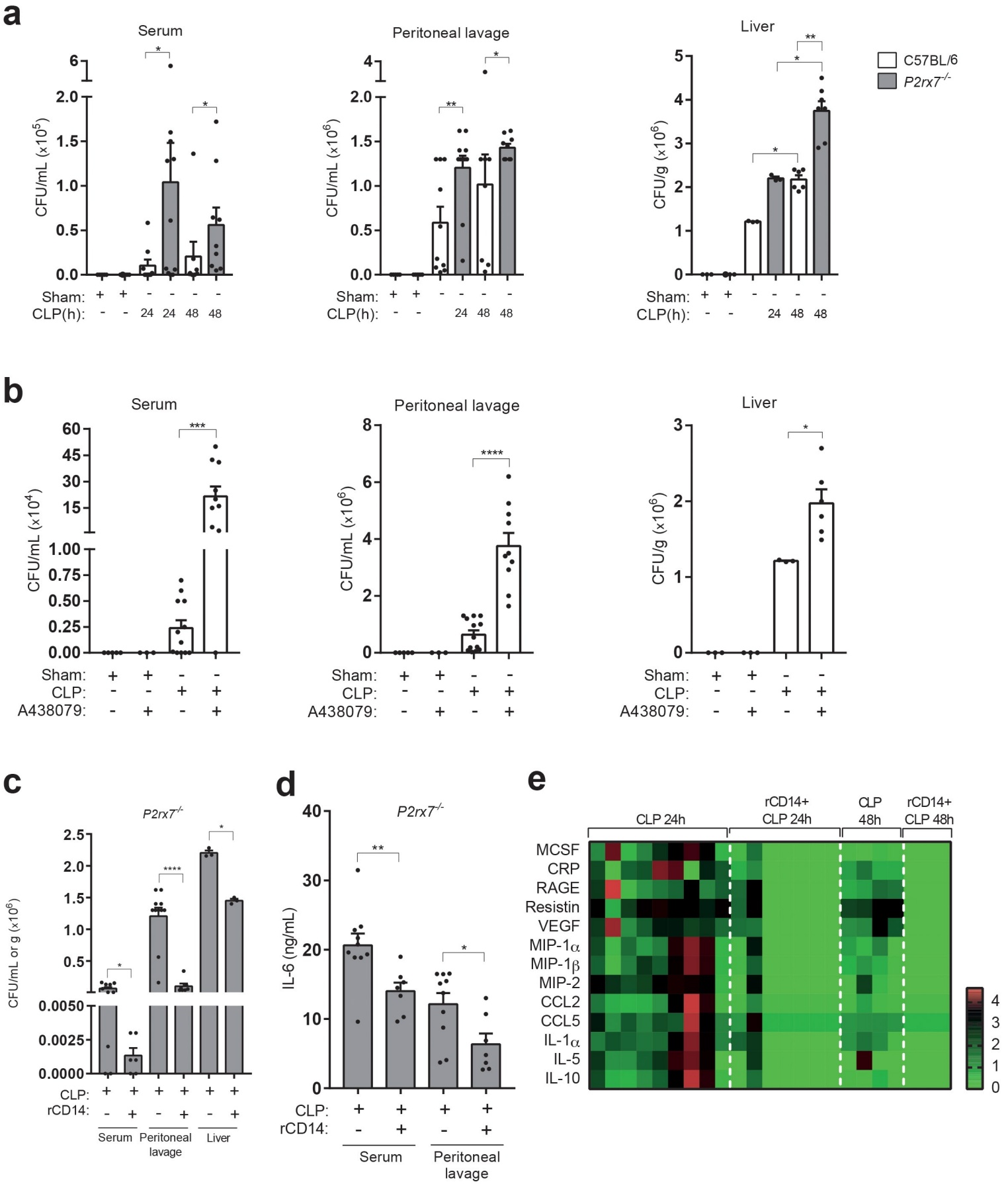
a
Serum
Peritoneal lavage
Liver
C57BL/6
P2rx7-/-
CFU/mL (x10^5)
CFU/mL (x10^6)
CFU/g (x10^6)
Sham:
CLP(h):
24 24 48 48
b
CFU/mL (x10^4)
CLP:
A438079:
c
P2rx7-/-
CFU/mL or g (x10^6)
rCD14:
Serum
Peritoneal lavage
Liver
d
IL-6 (ng/mL)
e
CLP 24h
rCD14+ CLP 24h
CLP 48h
rCD14+ CLP 48h
MCSF
CRP
RAGE
Resistin
VEGF
MIP-1α
MIP-1β
MIP-2
CCL2
CCL5
IL-1α
IL-5
IL-10

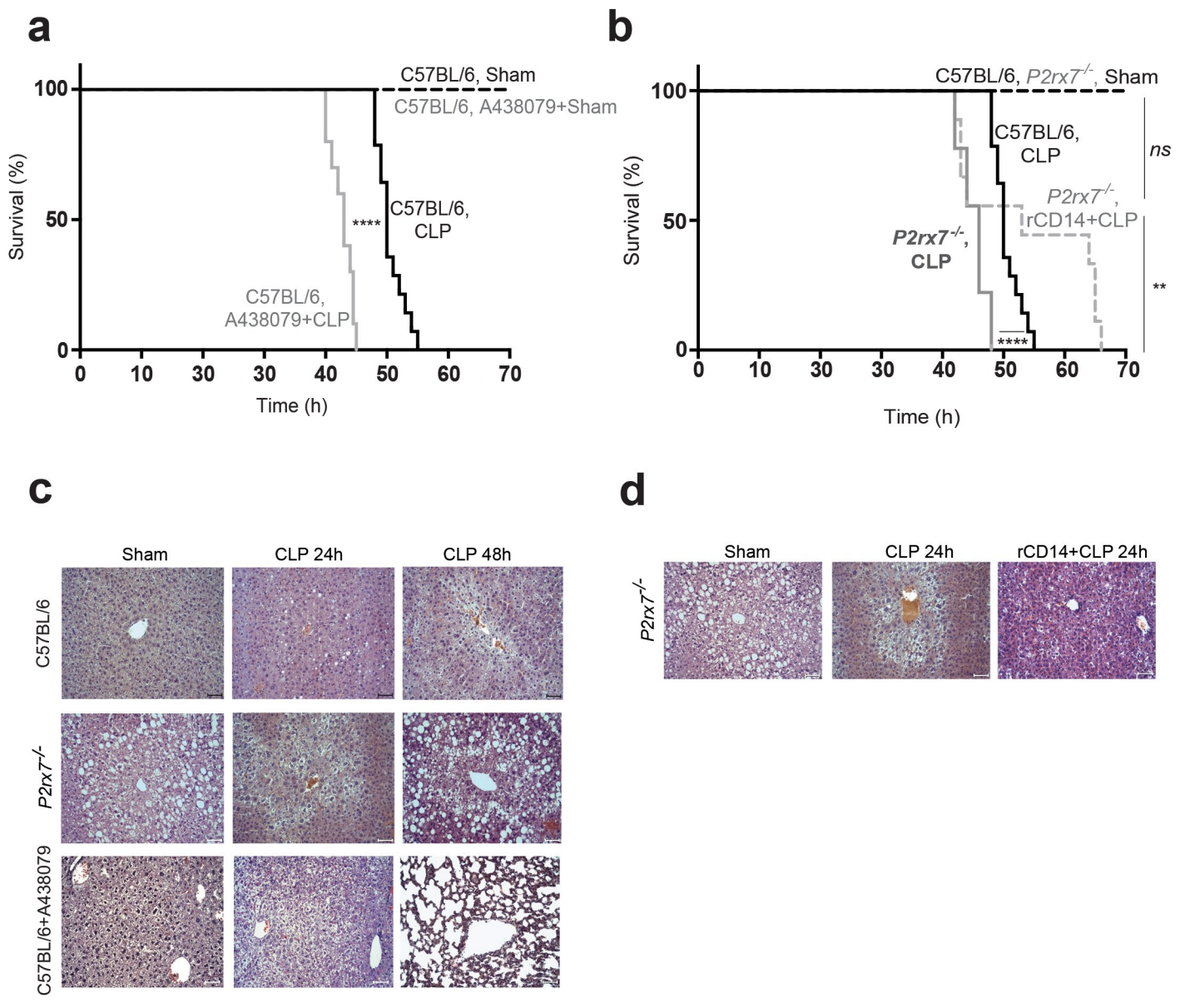
a
C57BL/6, Sham
C57BL/6, A438079+Sham
C57BL/6,
CLP
****
C57BL/6,
A438079+CLP
Survival (%)
Time (h)
b
C57BL/6, P2rx7-/-, Sham
C57BL/6,
CLP
ns
P2rx7-/-,
rCD14+CLP
P2rx7-/-,
CLP
**
****
Survival (%)
Time (h)
c
Sham
CLP 24h
CLP 48h
C57BL/6
P2rx7-/-
C57BL/6+A438079
d
Sham
CLP 24h
rCD14+CLP 24h
P2rx7-/-

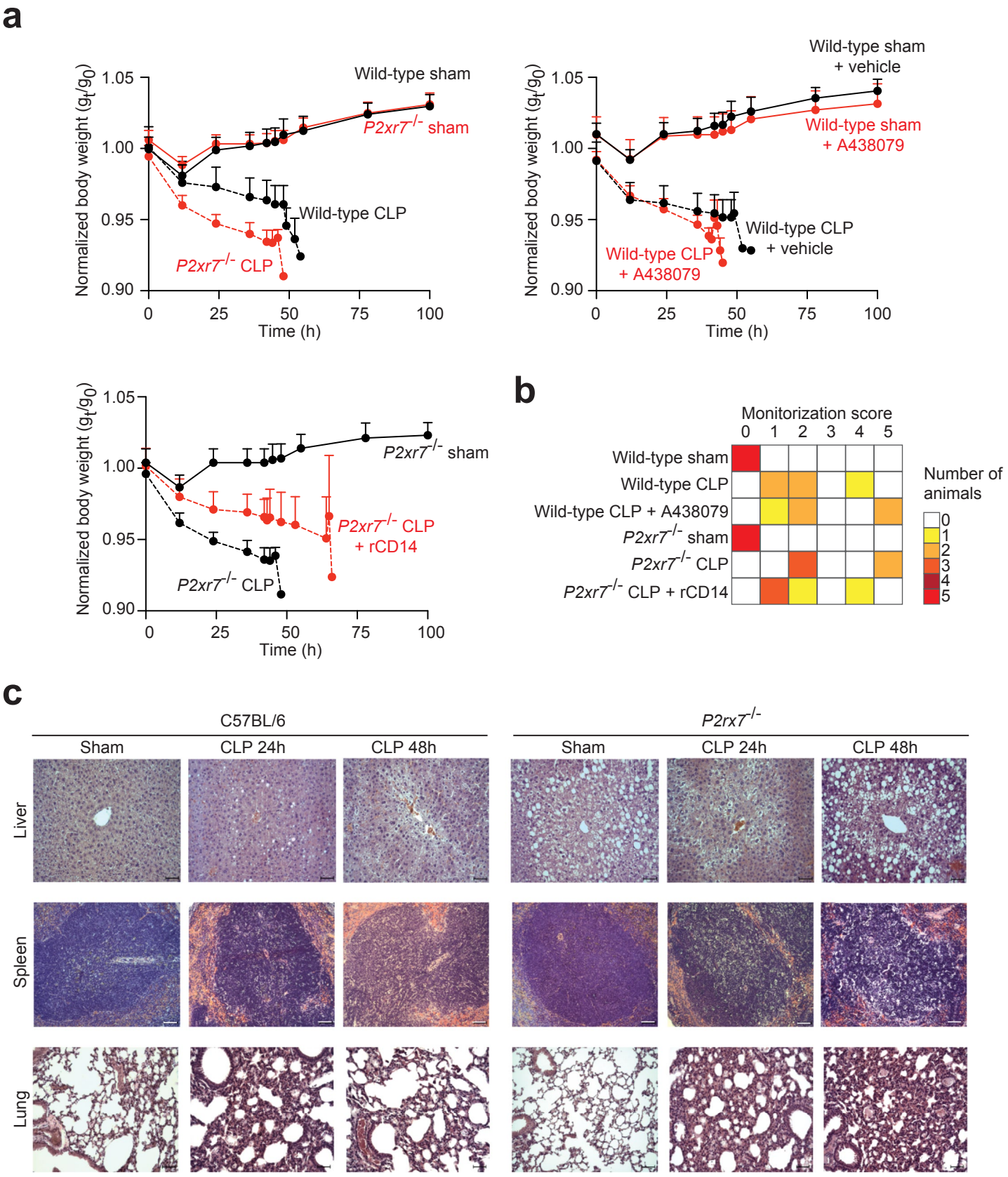
a
Normalized body weight ($g_t/g_0$)
1.05
1.00
0.95
0.90
0
25
50
75
100
Time (h)
Wild-type sham
P2xr7-/- sham
Wild-type CLP
P2xr7-/- CLP
Wild-type sham + vehicle
Wild-type sham + A438079
Wild-type CLP + vehicle
Wild-type CLP + A438079
P2xr7-/- CLP + rCD14
b
Monitorization score
0 1 2 3 4 5
Wild-type sham
Wild-type CLP
Wild-type CLP + A438079
P2xr7-/- sham
P2xr7-/- CLP
P2xr7-/- CLP + rCD14
Number of animals
0
1
2
3
4
5
c
C57BL/6
P2rx7-/-
Sham
CLP 24h
CLP 48h
Liver
Spleen
Lung

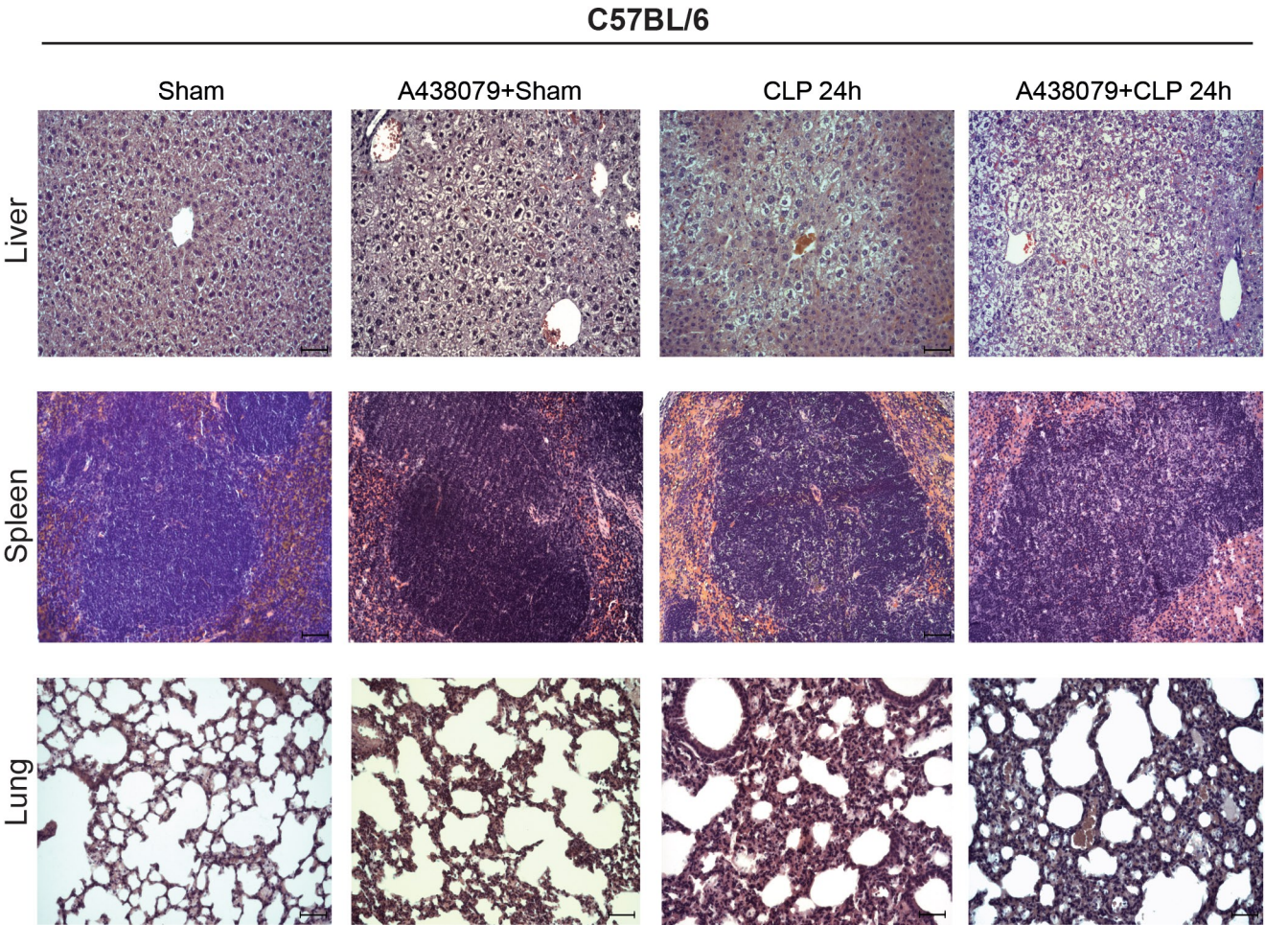
C57BL/6
Sham
A438079+Sham
CLP 24h
A438079+CLP 24h
Liver
Spleen
Lung

## *P2rx7*$^{-/-}$